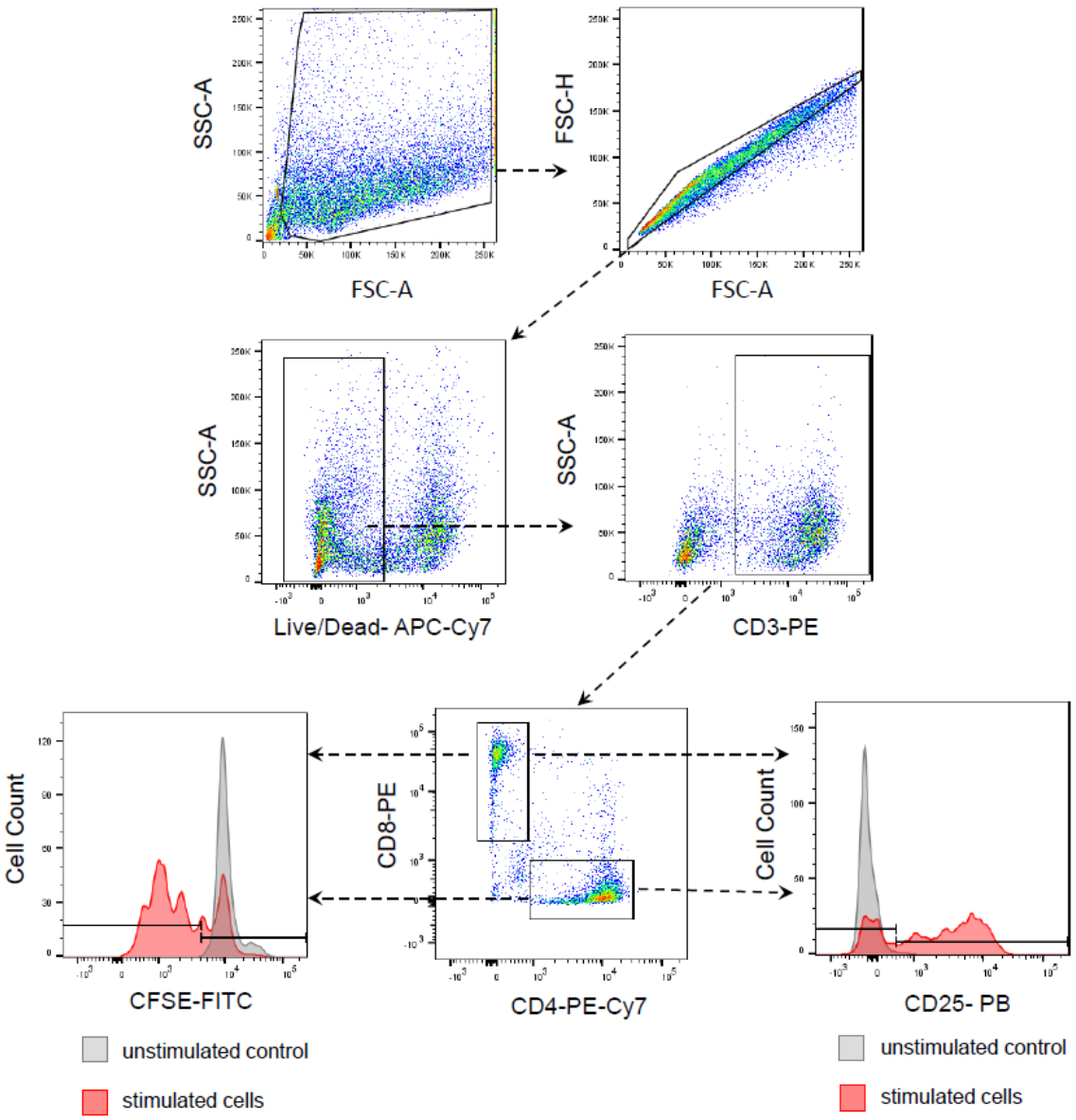

Fig. S1. Representative FACS gating strategy for quantifying functional immunosuppression. Cells were first gated on a SSC-A vs. FSC-A plot to exclude debris. Single cells were then gated based on a FSC-H vs. FSC-A plot. Live cells were then gated using fixable live/dead stain. The percentage of each T-cell subset was then determined based on CD3, CD4, and CD8 staining. The percentage of proliferating T-cells was determined based on CFSE staining and the percentage of activated T-cells was determined based on CD25 staining with respect to unstimulated cells.

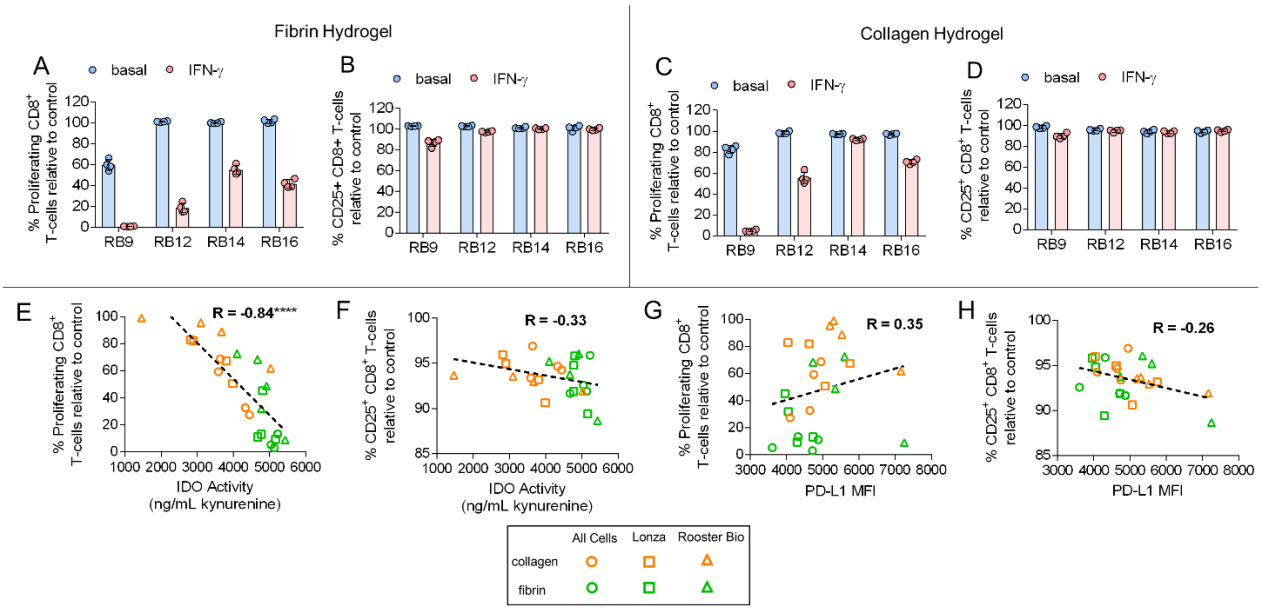

Fig. S2. Functional immunosuppressive capacity of IFN-γ licensed MSCs on biomaterial hydrogels. (A and B) (A) The percent proliferating and (B) percent $CD25^+$ $CD8^+$ T-cells in the presence of MSC lines, with and without IFN-γ licensing, cultured on fibrin. (C and D) (C) The percent proliferating and (D) percent $CD25^+$ $CD8^+$ T-cells in the presence of MSC lines, with and without IFN-γ licensing, cultured on collagen. (E and F) Correlation between IDO activity with (I) proliferating $CD8^+$ T-cells and (J) $CD25^+$ $CD8^+$ T-cells of IFN-γ licensed MSC cell lines cultured on fibrin and collagen. (G and H) Correlation between PD-L1 MFI with (G) proliferating $CD8^+$ T-cells and (H) $CD25^+$ $CD8^+$ T-cells of IFN-γ licensed MSC cell lines cultured on fibrin and collagen. Data are presented as means ± SD. Significance is denoted b $^{****}P \leq 0.0001$ by two-tailed Spearman's rank correlation.

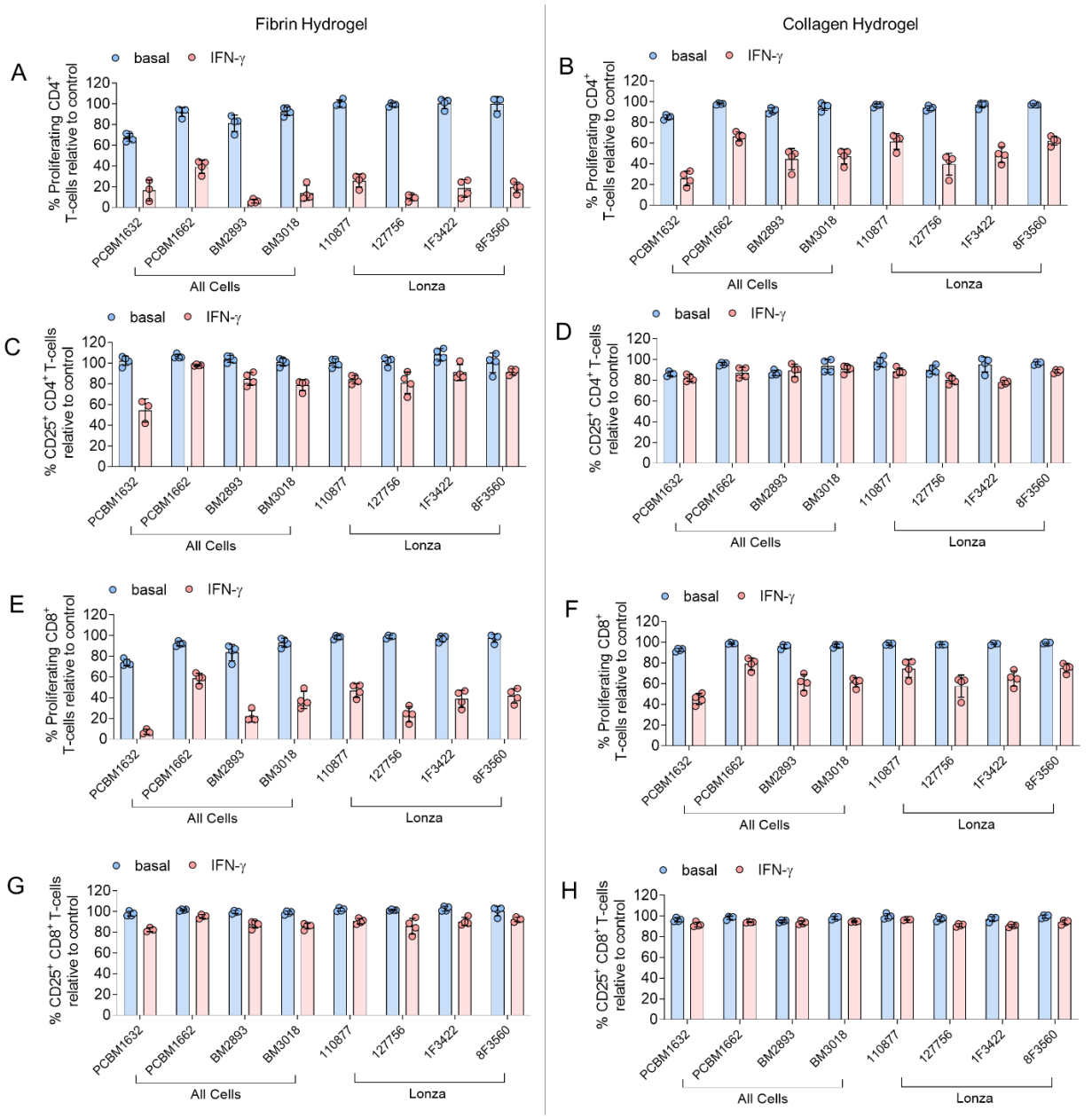

Fig. S3. Functional immunosuppressive capacity of IFN-γ licensed MSCs from All Cells and Lonza on biomaterial hydrogels. (A and B) The percent proliferating $CD4^+$ T-cells in the presence of MSC lines, with and without IFN-γ licensing, cultured on (A) fibrin and (B) collagen. (C and D) The percent $CD25^+$ $CD4^+$ T-cells in the presence of MSC lines, with and without IFN-γ licensing, cultured on (C) fibrin and (D) collagen. (E and F) The percent proliferating $CD8^+$ T-cells in the presence of MSC lines, with and without IFN-γ licensing, cultured on (E) fibrin and (F) collagen. (G and H) The percent $CD25^+$ $CD8^+$ T-cells in the presence of MSC lines, with and without IFN-γ licensing, cultured on (G) fibrin and (H) collagen. Data are presented as means ± SD.

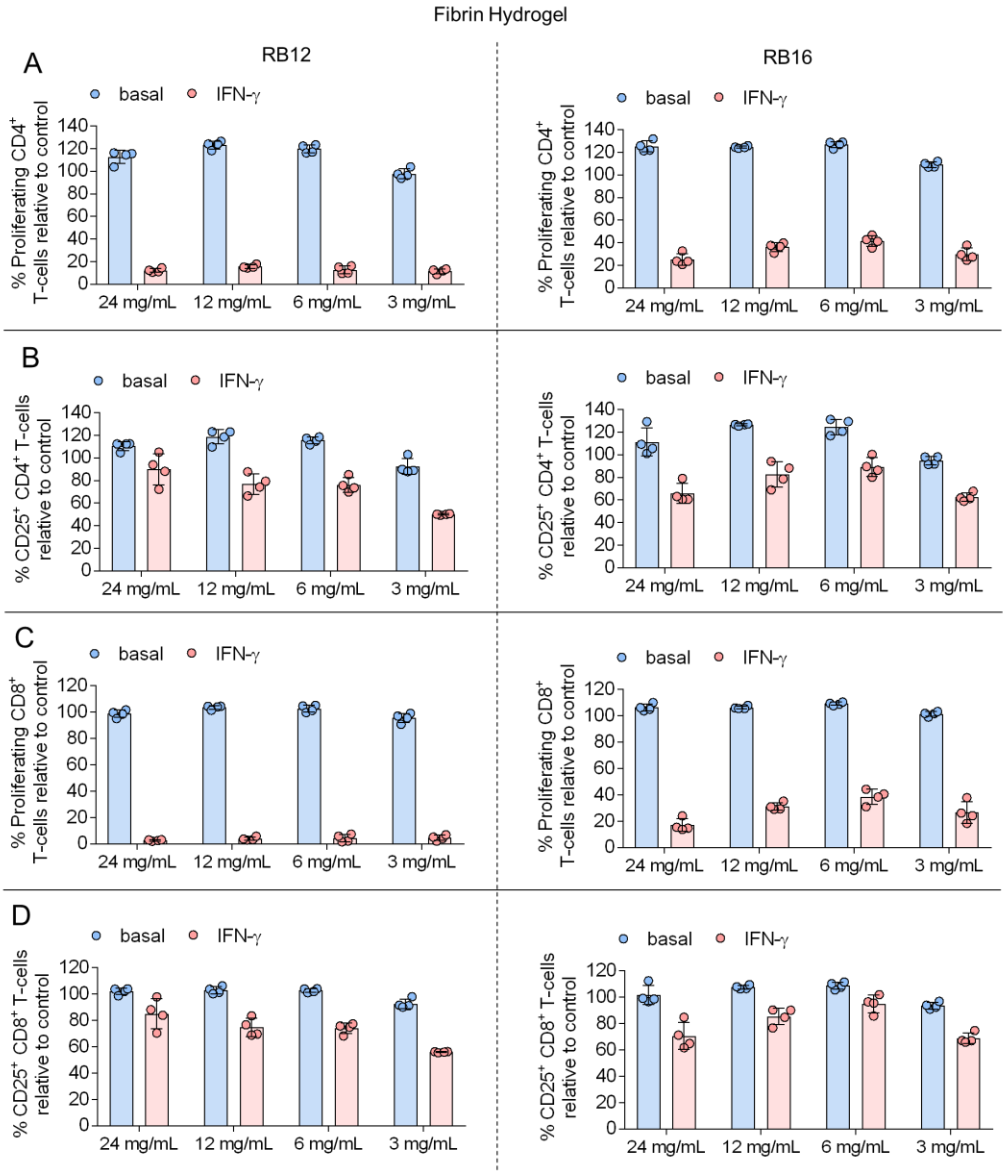

Fig. S4. Role of fibrinogen concentration on IFN-γ licensed MSC immunosuppressive capacity on fibrin hydrogels. (A and B) (A) The percent proliferating and (B) percent $CD25^+$ $CD4^+$ T-cells in the presence of MSC lines, with and without IFN-γ licensing, cultured on fibrin hydrogels of varying fibrinogen polymer concentrations. (C and D) (C) The percent proliferating and (D) percent $CD25^+$ $CD8^+$ T-cells in the presence of MSC lines, with and without IFN-γ licensing, cultured on fibrin hydrogels of varying fibrinogen polymer concentrations. Data are presented as means ± SD.

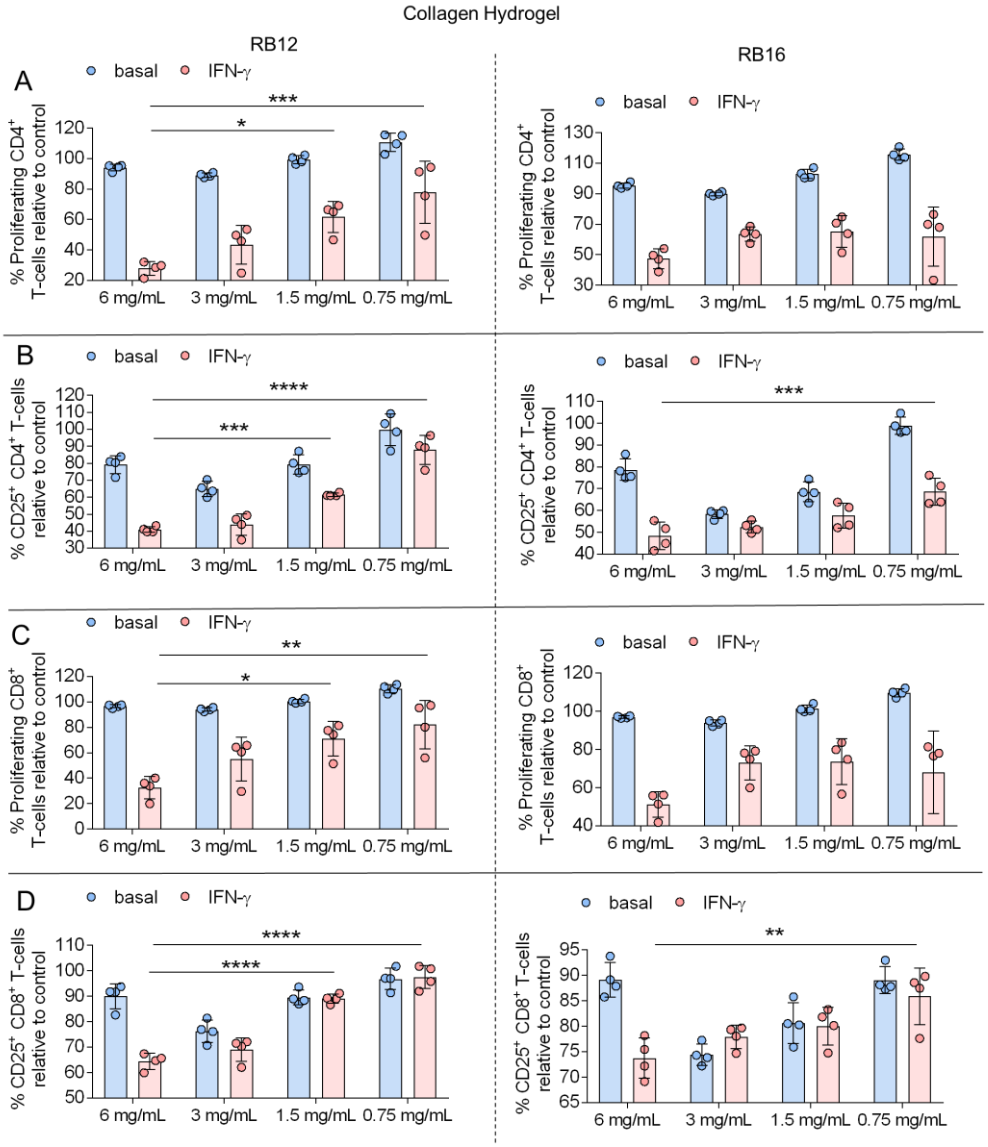

Fig. S5. Role of collagen I concentration on IFN-γ licensed MSC immunosuppressive capacity on collagen hydrogels. (A and B) (A) The percent proliferating and (B) percent $CD25^+$ $CD4^+$ T-cells in the presence of MSC lines, with and without IFN-γ licensing, cultured on collagen hydrogels of varying collagen I polymer concentrations. (C and D) (C) The percent proliferating and (D) percent $CD25^+$ $CD8^+$ T-cells in the presence of MSC lines, with and without IFN-γ licensing, cultured on collagen hydrogels of varying collagen I polymer concentrations. Data are presented as means ± SD. Significance is denoted by $*P \leq 0.05$, $**P \leq 0.01$, $***P \leq 0.001$, or $****P \leq 0.0001$ by one-way analysis of variance (ANOVA) with Tukey's post hoc test.

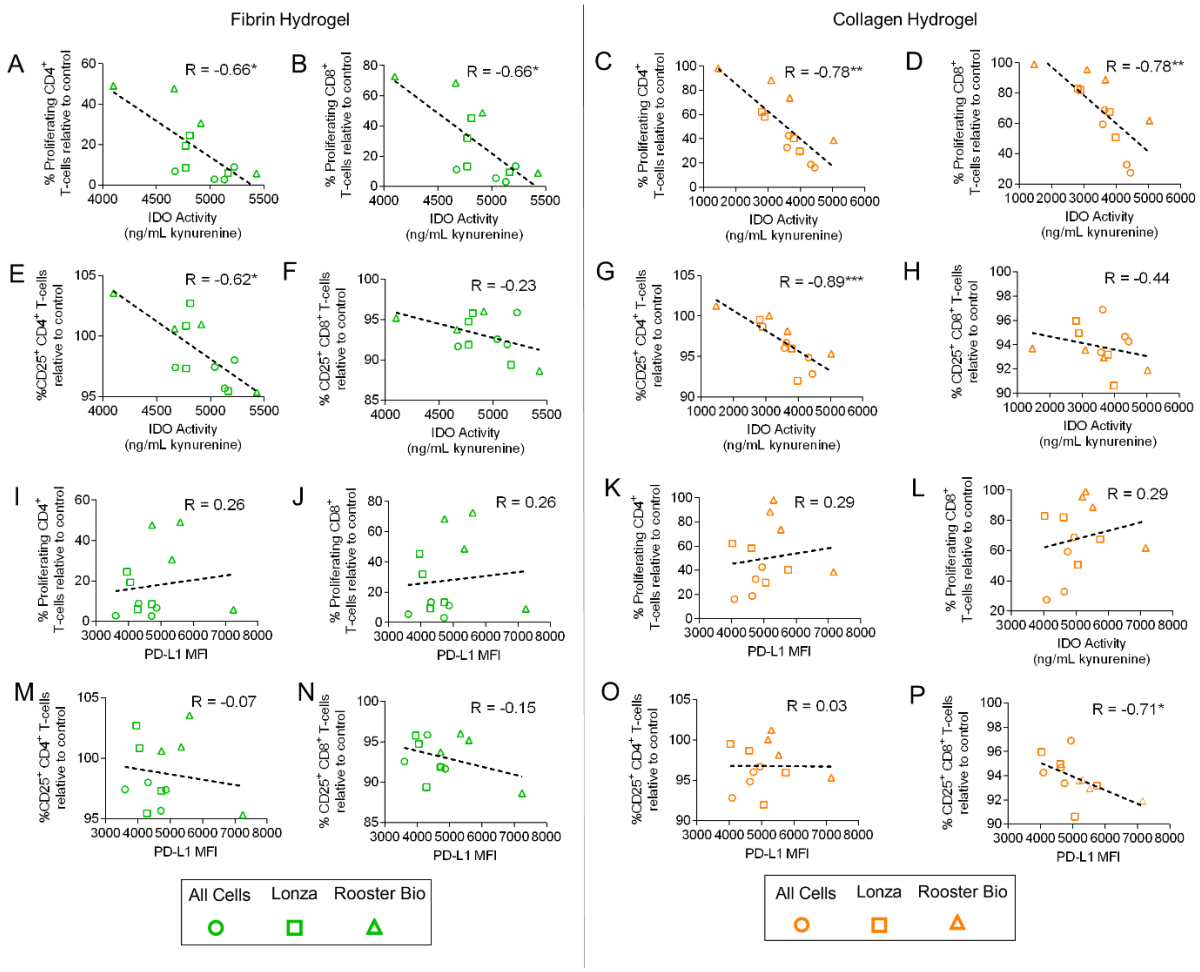

Fig. S6. IDO activity correlates with functional immunosuppressive capacity of IFN-γ licensed MSCs on biomaterials. (A to D) Correlation of IDO activity with percent proliferating (A) $CD4^+$ and (B) $CD8^+$ T-cells of IFN-γ licensed MSCs cultured on fibrin, and with percent proliferating (C) $CD4^+$ and (D) $CD8^+$ T-cells of IFN-γ licensed MSCs cultured on collagen. (E to H) Correlation of IDO activity with percent $CD25^+$ (E) $CD4^+$ and (F) $CD8^+$ T-cells of IFN-γ licensed MSCs cultured on fibrin, and with percent $CD25^+$ (G) $CD4^+$ and (H) $CD8^+$ T-cells of IFN-γ licensed MSCs cultured on collagen. (I to L) Correlation of mean fluorescence intensity (MFI) of PD-L1 expression with percent proliferating (I) $CD4^+$ and (J) $CD8^+$ T-cells of IFN-γ licensed MSCs cultured on fibrin, and with percent proliferating (K) $CD4^+$ and (L) $CD8^+$ T-cells of IFN-γ licensed MSCs cultured on collagen. (M to P) Correlation of mean fluorescence intensity (MFI) of PD-L1 expression with percent $CD25^+$ (M) $CD4^+$ and (N) $CD8^+$ T-cells of IFN-γ licensed MSCs cultured on fibrin, and with percent $CD25^+$ (O) $CD4^+$ and (P) $CD8^+$ T-cells of IFN-γ licensed MSCs cultured on collagen. Data are presented as means ± SD. Significance is denoted by $*P \leq 0.05$ or $**P \leq 0.01$ by two-tailed Spearman's rank correlation.

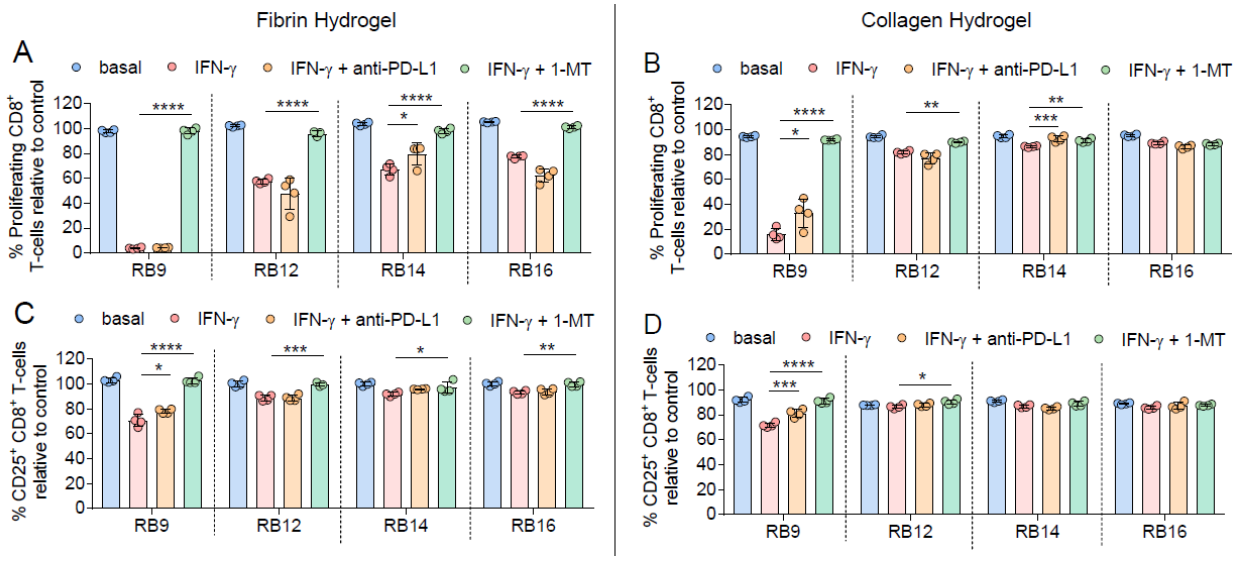

Fig. S7. IDO activity strongly regulates functional immunosuppressive capacity of IFN-γ licensed MSCs on biomaterials. (A and B) The percent proliferating $CD8^+$ T-cells in the presence of MSC lines, with and without IFN-γ licensing, cultured on (A) fibrin or (B) collagen with and without the addition of anti-PD-L1 antibody or 1-methyl-DL-tryptophan (1-MT), an IDO inhibitor. (C and D) The percent $CD25^+$ $CD8^+$ T-cells in the presence of MSC lines, with and without IFN-γ licensing, cultured on (C) fibrin or (D) collagen with and without the addition of anti-PD-L1 antibody or 1-MT. n = 3-4 for all data sets. Data are presented as means ± SD. Significance is denoted by $*P \leq 0.05$, $**P \leq 0.01$, $***P \leq 0.001$, or $****P \leq 0.0001$ by one-way analysis of variance (ANOVA) with Tukey's post hoc test; separate comparisons were made between conditions of each cell line.

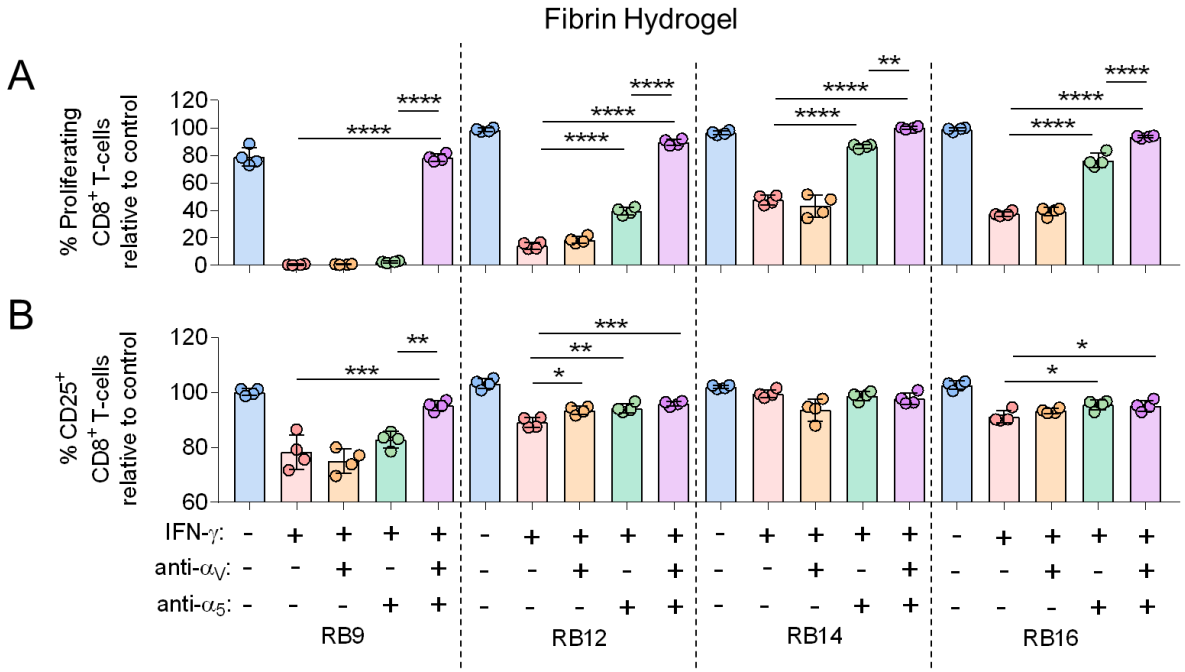

Fig. S8. Engagement of α_V and α_5 integrins regulates immunosuppressive capacity of IFN-γ licensed MSCs on fibrin. (A and B) (A) The percent proliferating and (B) $CD25^+$ $CD8^+$ T-cells in the presence of various MSCs lines, with and without IFN-γ licensing, cultured on fibrin, with and without the addition of inhibitors to α_V and/or α_5 integrin binding. Labels for groups in (A-B) are shown in (B). n = 4 for all data sets. Data are presented as means ± SD. Significance is denoted by $*P \leq 0.05$, $**P \leq 0.01$, $***P \leq 0.001$, or $****P \leq 0.0001$ by one-way analysis of variance (ANOVA) with Tukey's post hoc test; separate comparisons were made between conditions of each cell line.

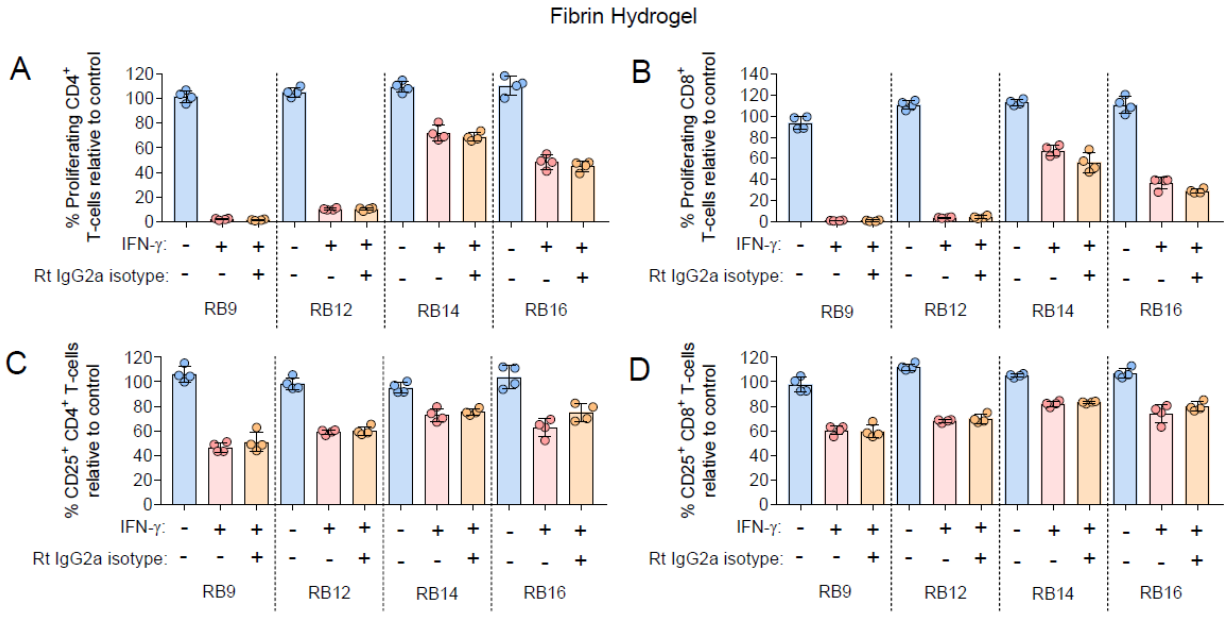

Fig. S9. Role of RGD integrin isotype antibodies on immunosuppressive capacity of IFN-γ licensed MSCs on fibrin. (A and B) The percent proliferating (A) $CD4^+$ and (B) $CD8^+$ T-cells in the presence of MSC lines, cultured on fibrin with and without IFN-γ stimulation and the addition of a rat IgG2a isotype control antibody. (C and D) The percent $CD25^+$ (C) $CD4^+$ and (D) $CD8^+$ T-cells in the presence of MSC lines, cultured on fibrin with and without IFN-γ stimulation and the addition of a rat IgG2a isotype control antibody. Data are presented as means ± SD.

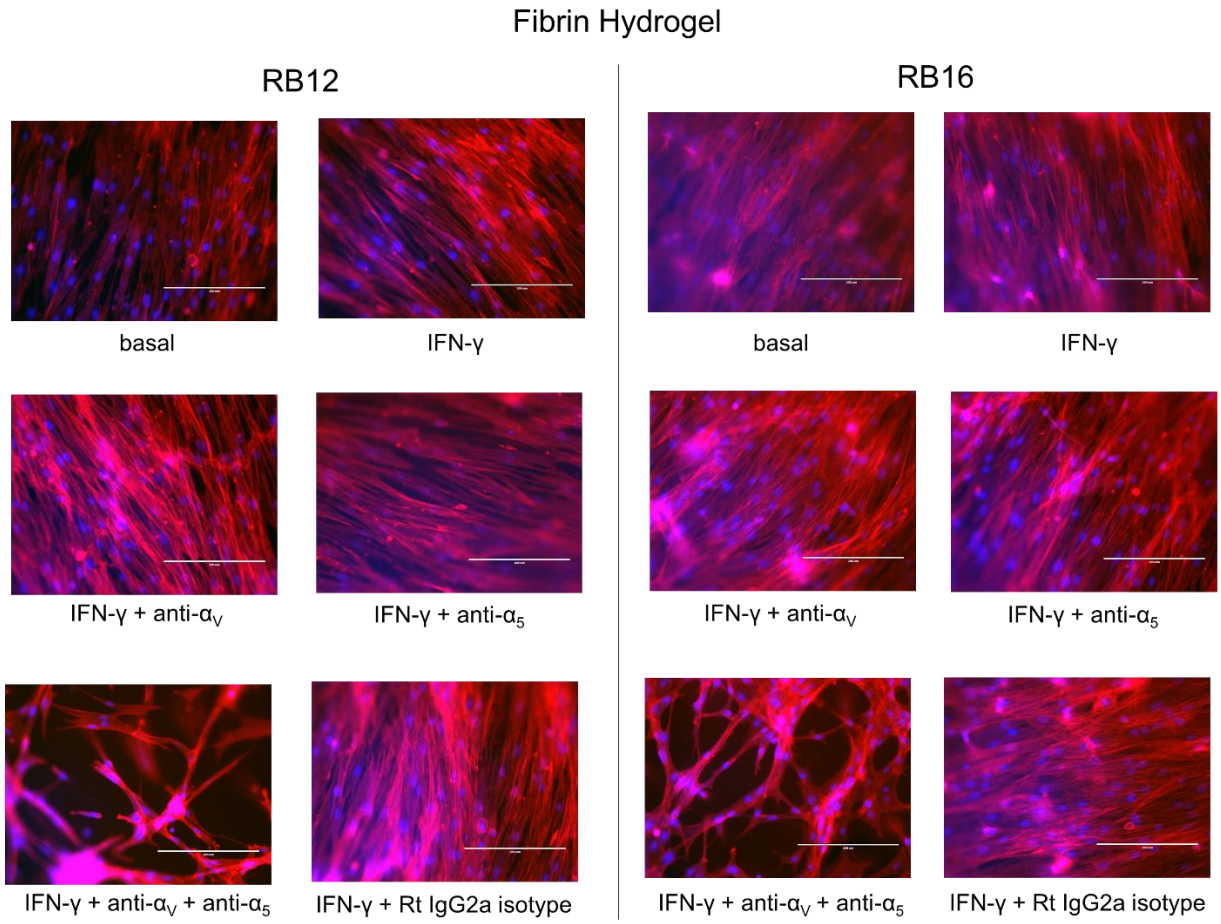

Fig. S10. Engagement of α_V and α_5 integrins regulates morphology of IFN-γ licensed MSCs on fibrin. Representative images showing MSCs cultured on fibrin hydrogels in the presence of basal media, IFN-γ licensing, IFN-γ licensing with α_V inhibitor, IFN-γ licensing with α_5 inhibitor, IFN-γ licensing with α_V + α_5 inhibitors, or IFN-γ licensing with rat IgG2a isotype control antibody. Blue = DAPI, Red = phalloidin F-actin staining, Scale Bar = 200 μm.

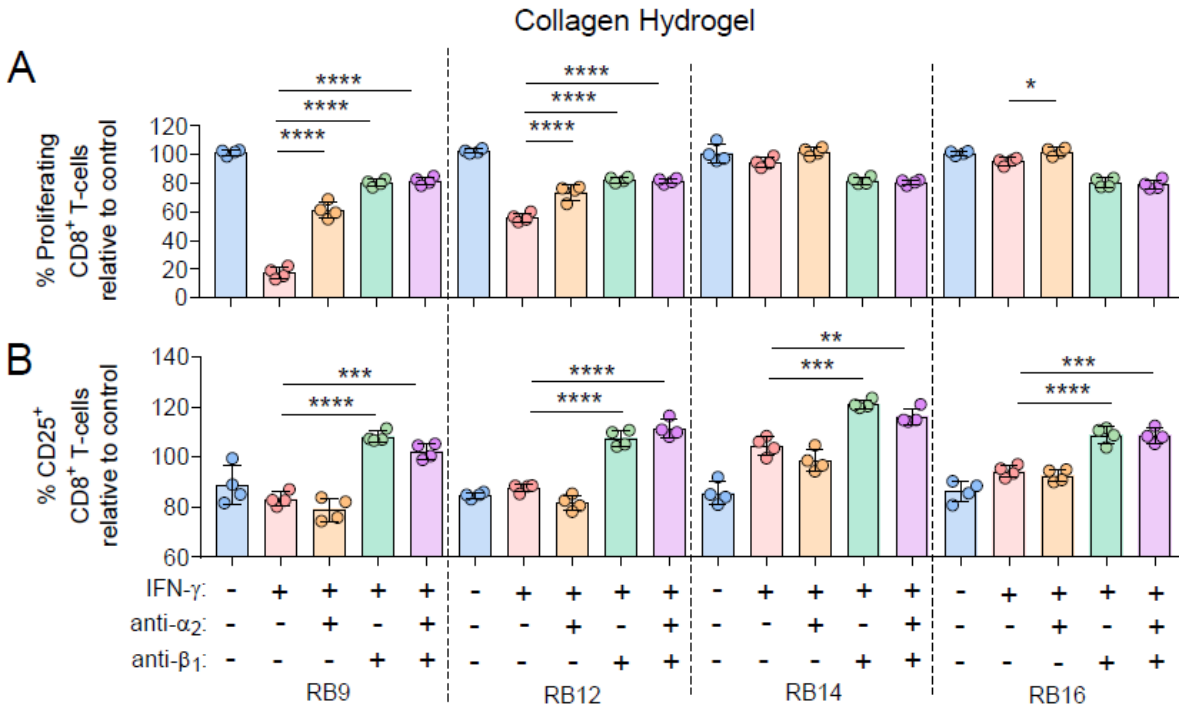

Fig. S11. Engagement of α_2 and β_1 integrins regulates immunosuppressive capacity of IFN-γ licensed MSCs on collagen. (A and B) (A) The percent proliferating and (B) $CD25^+$ $CD8^+$ T-cells in the presence of various MSCs lines, with and without IFN-γ licensing, cultured on collagen, with and without the addition of inhibitors to α_2 and/or β_1 integrin binding. Labels for groups in (A-B) are shown in (B). n = 4 for all data sets. Data are presented as means ± SD. Significance is denoted by $*P \leq 0.05$, $**P \leq 0.01$, $***P \leq 0.001$, or $****P \leq 0.0001$ by one-way analysis of variance (ANOVA) with Tukey's post hoc test; separate comparisons were made between conditions of each donor.

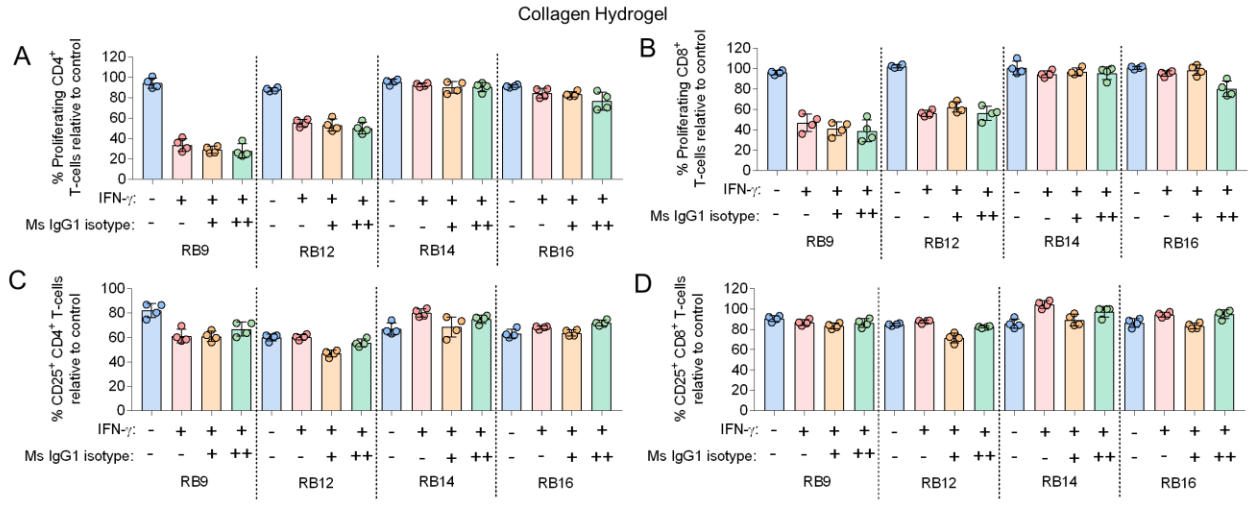

Fig. S12. Role of collagen integrin isotype antibodies on immunosuppressive capacity of IFN-γ licensed MSCs on collagen. (A and B) The percent proliferating (A) $CD4^+$ and (B) $CD8^+$ T-cells in the presence of MSC lines, cultured on collagen with and without IFN-γ licensing and the addition of varying concentrations of mouse IgG1κ isotype control antibody. (C and D) The percent $CD25^+$ (C) $CD4^+$ and (D) $CD8^+$ T-cells in the presence of MSC lines, cultured on collagen with and without IFN-γ licensing and the addition of varying concentrations of mouse IgG1κ isotype control antibody. For the mouse IgG1κ isotype control antibody condition, '+' denotes 10 μg/mL and '++' denotes 20 μg/mL. 20 μg/mL of mouse IgG1κ isotype control antibody was tested as a control condition for adding both the anti-α_2 and anti-β_1 integrin blocking antibodies together. Data are presented as means ± SD.

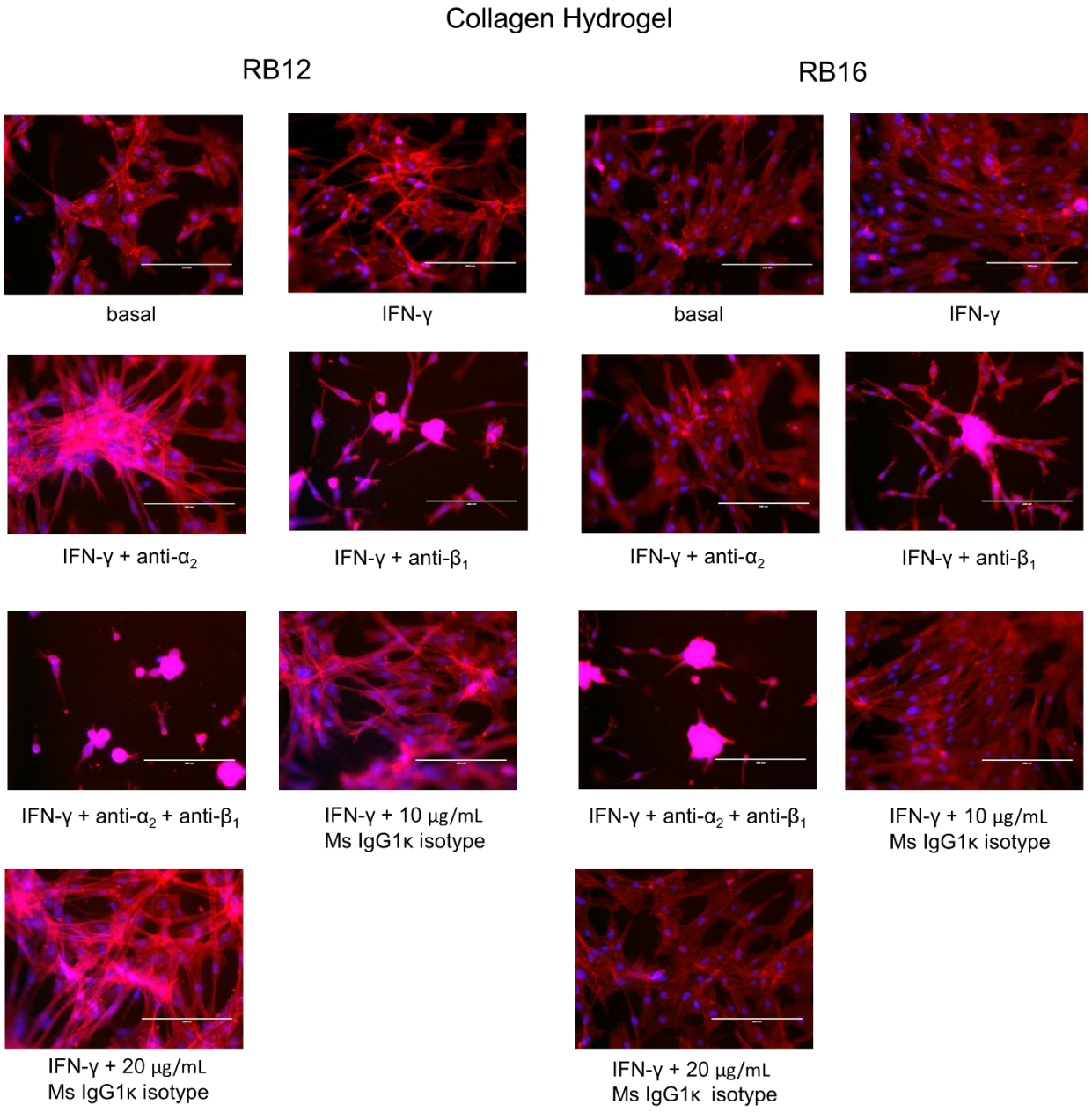

Fig. S13. Engagement of α_2 and β_1 integrins regulates morphology of IFN-γ licensed MSCs on collagen. Representative images showing MSCs cultured on collagen hydrogels in the presence of basal media, IFN-γ licensing, IFN-γ licensing with α_2 inhibitor, IFN-γ licensing with β_1 inhibitor, IFN-γ licensing with $\alpha_2 + \beta_1$ inhibitors, IFN-γ licensing with 10 μg/mL mouse IgG1κ isotype control antibody, or IFN-γ licensing with 20 μg/mL mouse IgG1κ isotype control antibody. Blue = DAPI, Red = phalloidin F-actin staining, Scale Bar = 200 μm.

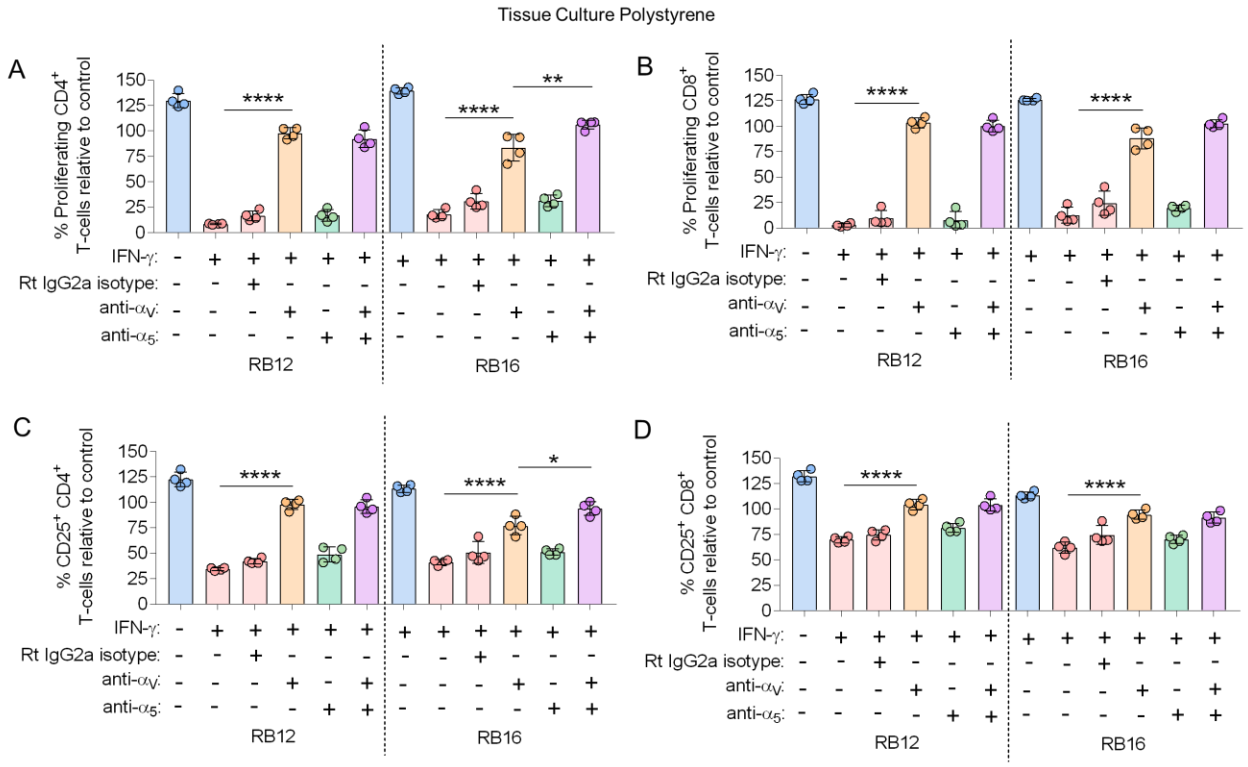

Fig. S14. Engagement of α_V and α_5 integrins regulates immunosuppressive capacity of IFN-γ licensed MSCs on tissue culture polystyrene. (A and B) The percent proliferating (A) $CD4^+$ and (B) $CD8^+$ T-cells in the presence of various MSC lines, with and without IFN-γ licensing, cultured on tissue culture polystyrene, with and without the addition of inhibitors to α_V and/or α_5 integrin binding or a rat IgG2a isotype control antibody. (C and D) The percent $CD25^+$ (C) $CD4^+$ and (D) $CD8^+$ T-cells in the presence of various MSC lines, with and without IFN-γ licensing, cultured on tissue culture polystyrene, with and without the addition of inhibitors to α_V and/or α_5 integrin binding or a rat IgG2a isotype control antibody. Data are presented as means ± SD. Significance is denoted by $*P \leq 0.05$, $**P \leq 0.01$, or $****P \leq 0.0001$ by one-way analysis of variance (ANOVA) with Tukey's post hoc test; separate comparisons were made between conditions of each cell line.

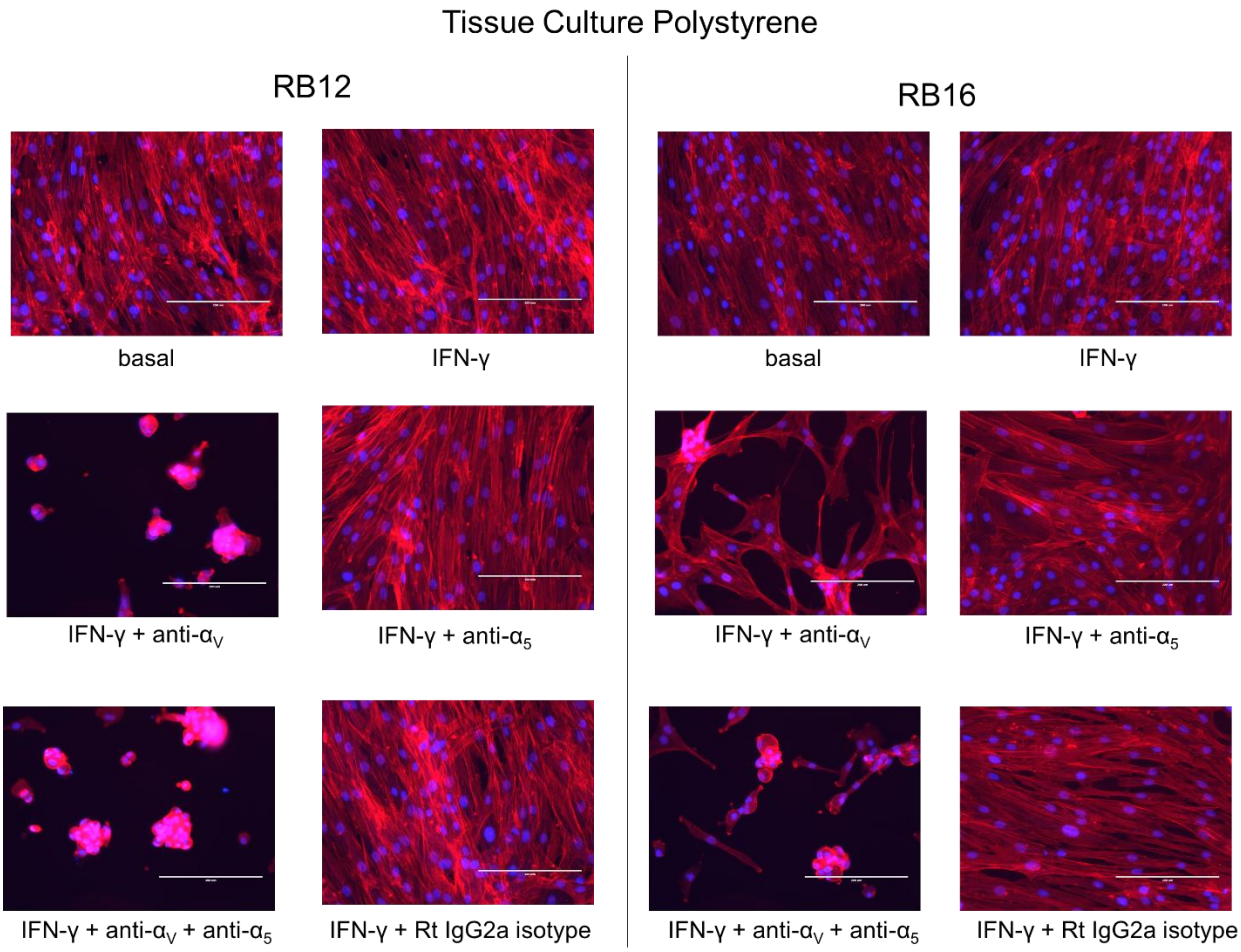

Fig. S15. Engagement of α_V and α_5 integrins regulates morphology of IFN-γ licensed MSCs on tissue culture polystyrene. Representative images showing MSCs cultured on tissue culture polystyrene in the presence of basal media, IFN-γ licensing, IFN-γ licensing with α_V inhibitor, IFN-γ licensing with α_5 inhibitor, IFN-γ licensing with $\alpha_V + \alpha_5$ inhibitors, or IFN-γ licensing with rat IgG2a isotype control antibody. Blue = DAPI, Red = phalloidin F-actin staining, Scale Bar = 200 μm.

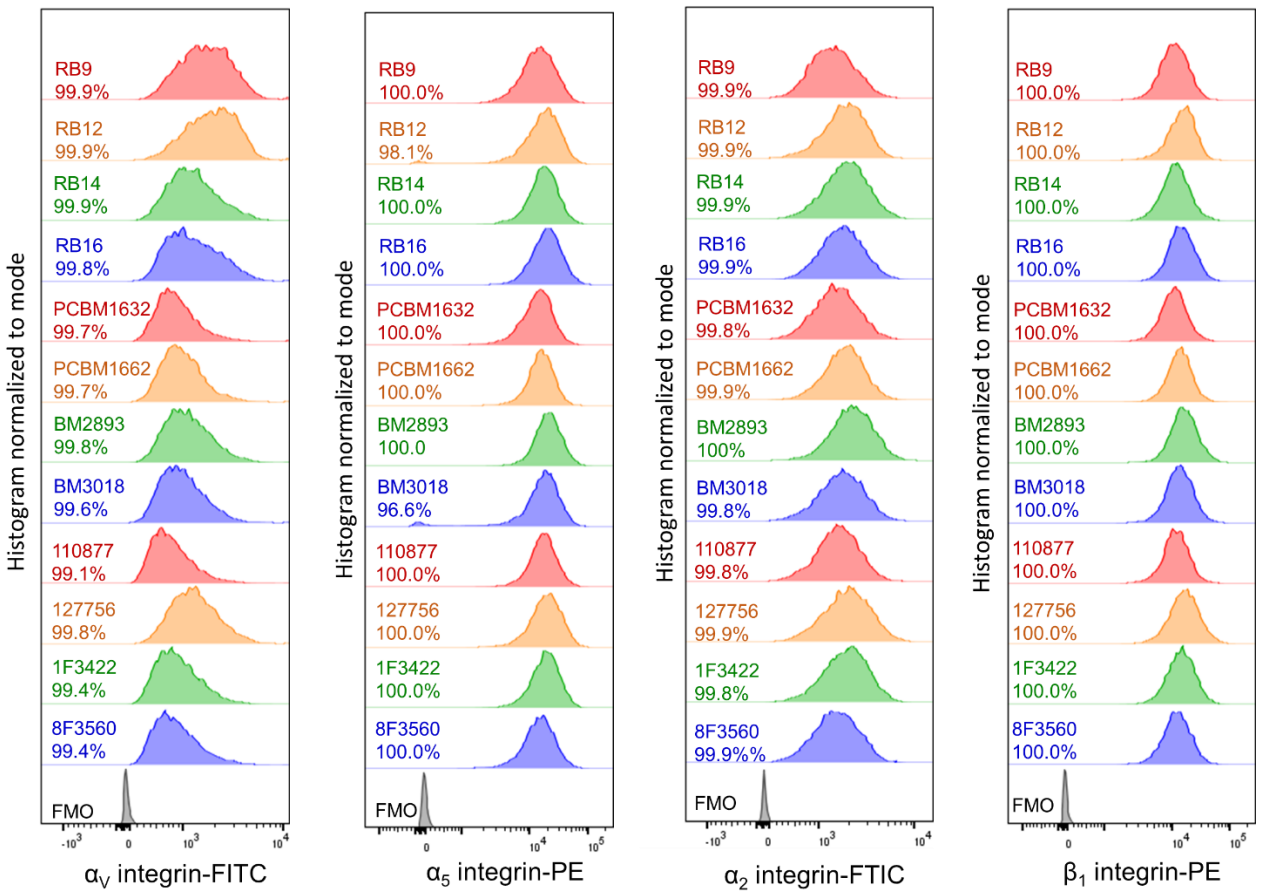

Fig. S16. FACS plots of α_V, α_5, α_2, and β_1 integrin expression for various, unlicensed MSC cell lines, denoting the percent positivity of each cell line.

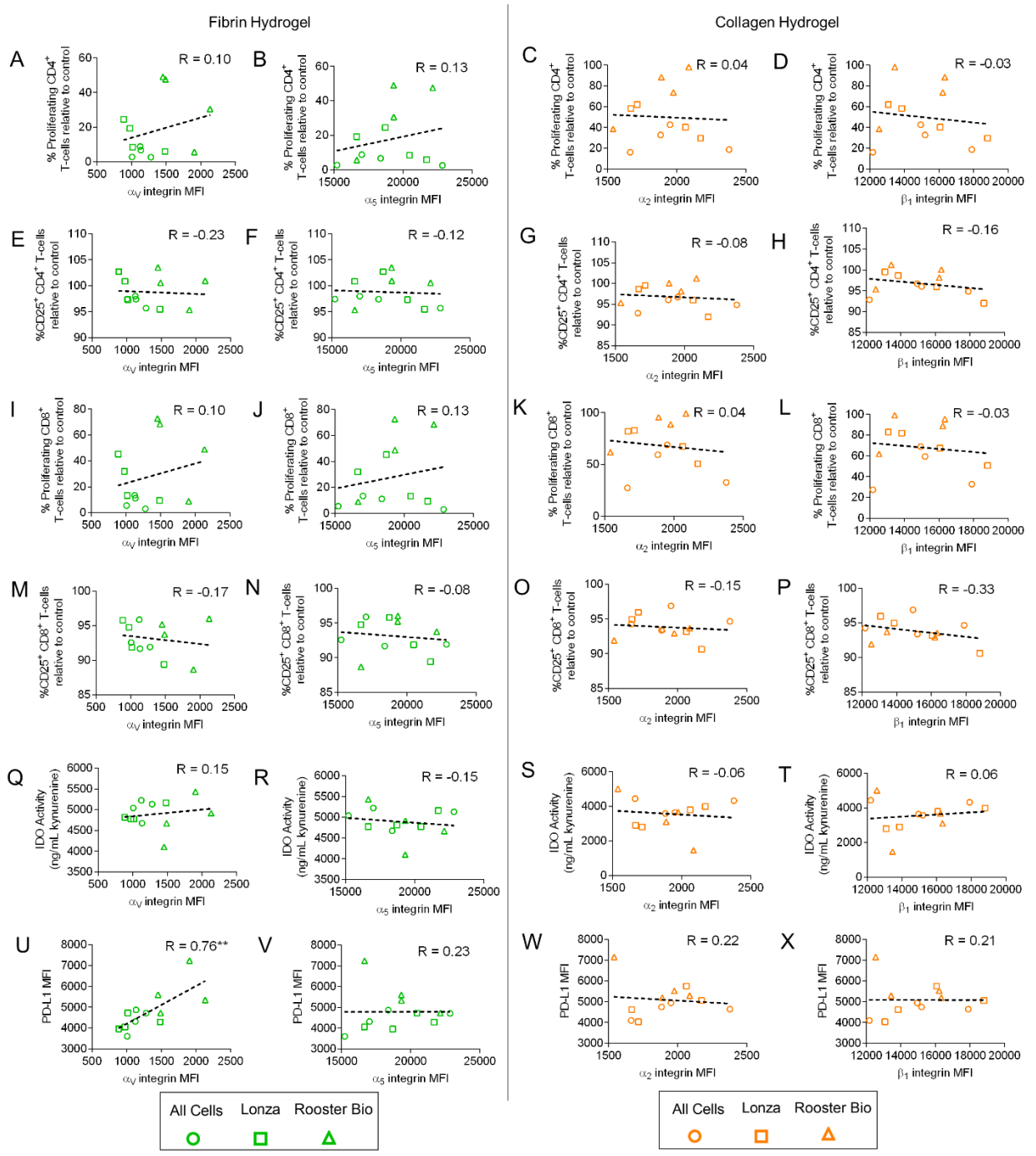

Fig. S17. Magnitude of integrin expression does not correlate with donor-to-donor variability of IFN-γ licensed MSC functional immunosuppressive capacity on biomaterials. (A to D) Correlation of percent proliferating $CD4^+$ T-cells in the presence of IFN-γ licensed MSC lines on (A,B) fibrin and (C,D) collagen with (A) α_V, (B) α_5, (C) α_2, and (D) β_1 integrin expression on MSC lines. (E to H) Correlation of $CD25^+$ $CD4^+$ T-cells in the presence of IFN-γ licensed MSC lines on (E,F) fibrin and (G,H) collagen with (E) α_V, (F) α_5, (G) α_2, and (H) β_1 integrin expression on MSC lines. (I to L) Correlation of percent proliferating $CD8^+$ T-cells in the presence of IFN-γ licensed MSC lines on (I,J) fibrin and (K,L) collagen with (I) α_V, (J) α_5, (K) α_2, and (L) β_1 integrin expression on MSC lines. (M to P) Correlation of $CD25^+$ $CD8^+$ T-cells in the presence of IFN-γ

licensed MSC lines on (M,N) fibrin and (O,P) collagen with (M) α_V, (N) α_5, (O) α_2, and (P) β_1 integrin expression on MSC lines. (Q to T) Correlation of IDO activity of IFN-γ licensed MSC lines on (Q,R) fibrin and (S,T) collagen with (Q) α_V, (R) α_5, (S) α_2, and (T) β_1 integrin expression on MSC lines. (U to X) Correlation of PD-L1 mean fluorescence intensity (MFI) of IFN-γ licensed MSC lines on (U,V) fibrin and (W,X) collagen with (U) α_V, (V) α_5, (W) α_2, and (X) β_1 integrin expression on MSC lines. Significance is denoted by $*P \leq 0.05$ by two-tailed Spearman's rank correlation.

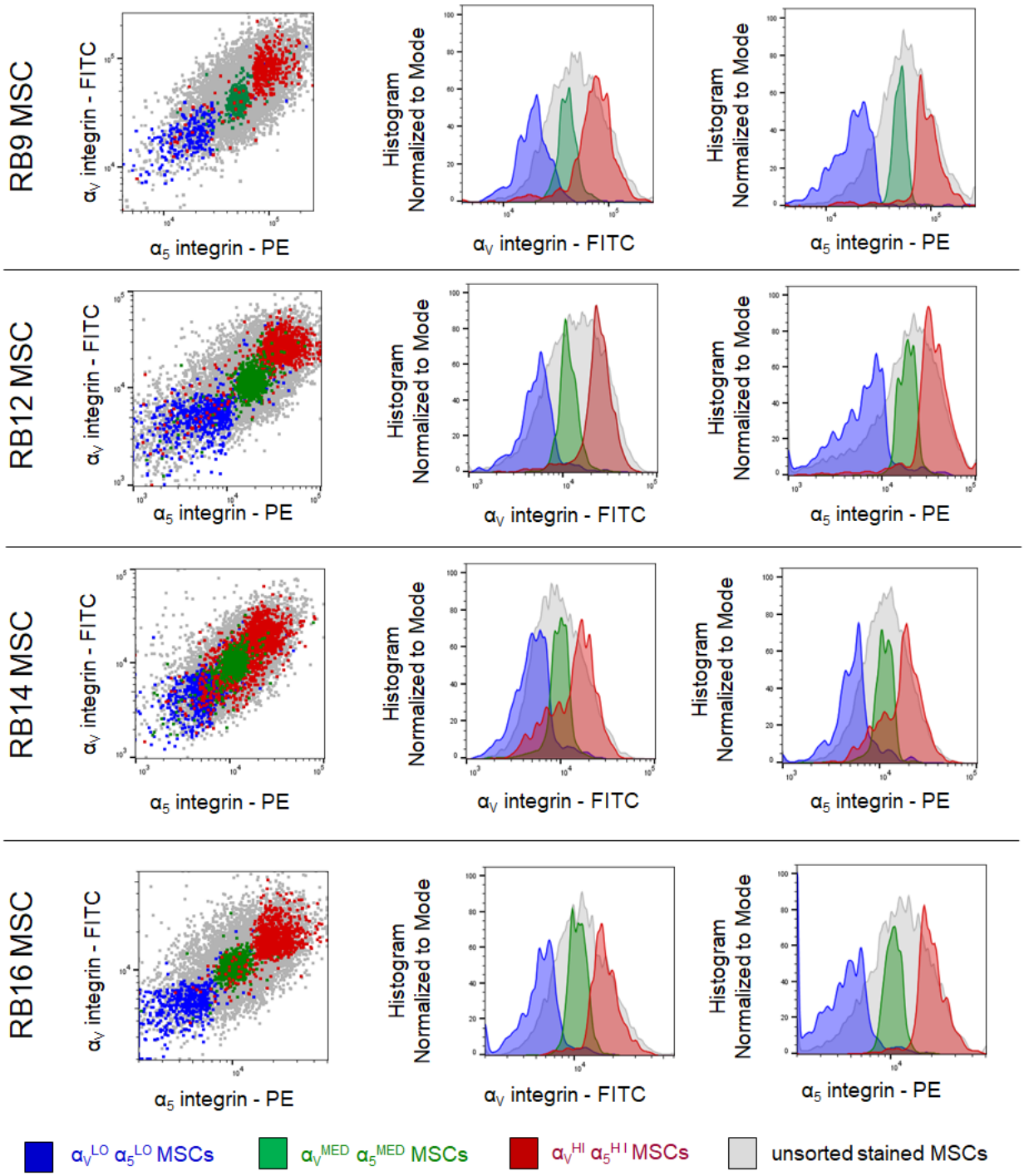

Fig. S18. FACS sorted MSCs by RGD integrins. Representative FACS plots of MSCs FACS sorted by magnitude of α_V and α_5 integrins for each MSC cell line.

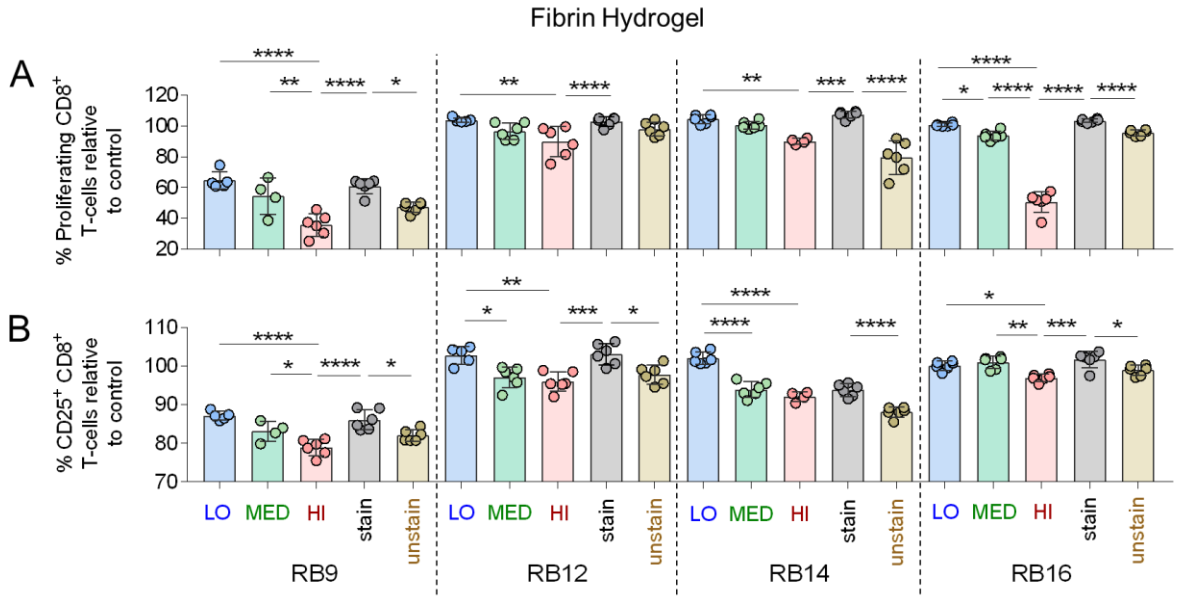

Fig. S19. Magnitude of α_V and α_5 integrins identifies MSC subpopulations of varying immunosuppressive capacity on fibrin hydrogels. (A) The percent proliferating and (B) $CD25^+$ $CD8^+$ T-cells in the presence of FACS sorted or unsorted MSC lines with IFN-γ licensing, cultured on fibrin. Labels for groups in (A-B) are shown in (B), where 'LO' denotes $\alpha_V^{LO}\alpha_5^{LO}$ expressing MSCs, 'MED' denotes $\alpha_V^{MED}\alpha_5^{MED}$ expressing MSCs, 'HI' denotes $\alpha_V^{HI}\alpha_5^{HI}$ expressing MSCs, 'stain' denotes unsorted MSCs stained with FACS sorting antibodies, and 'unstain' denotes unsorted, unstained MSCs. n = 4-6 for all data sets. Data are presented as means ± SD. Significance is denoted by $*P \leq 0.05$, $**P \leq 0.01$, $***P \leq 0.001$, or $****P \leq 0.0001$ by one-way analysis of variance (ANOVA) with Tukey's post hoc test; separate comparisons were made between conditions of each cell line.

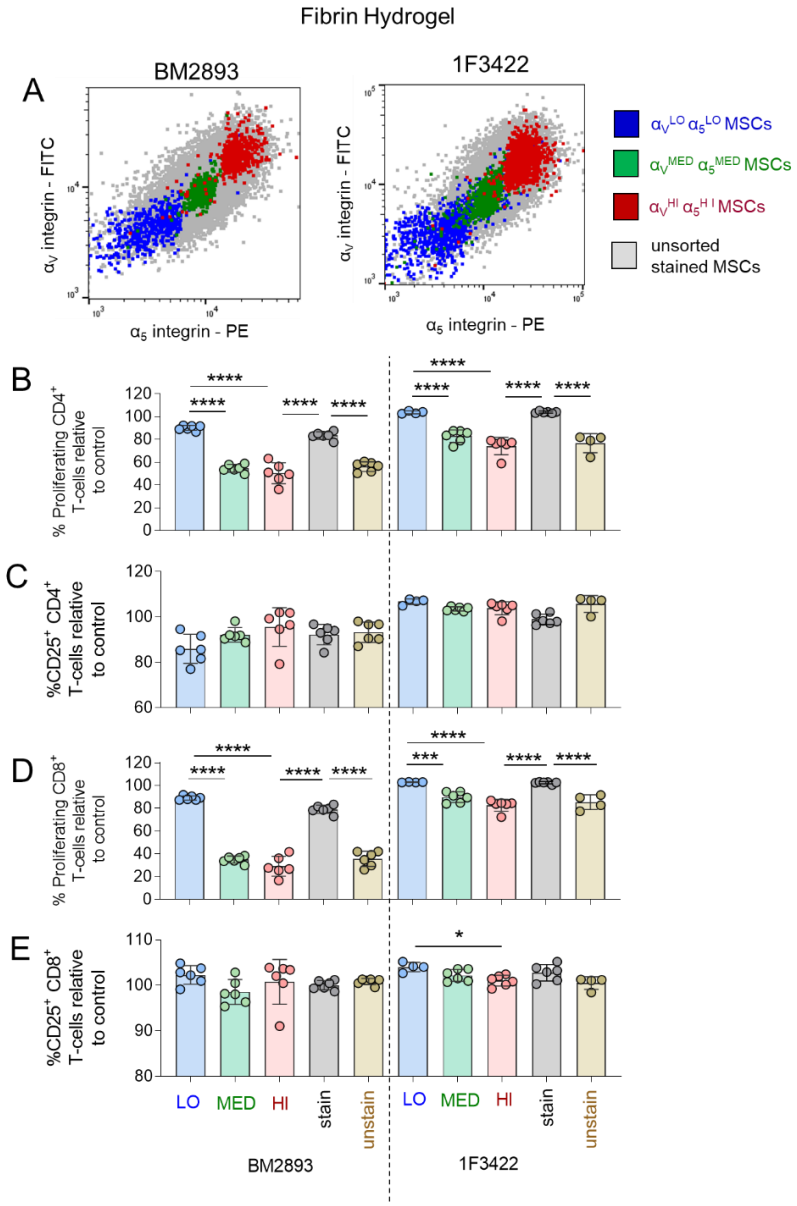

Fig. S20. Magnitude of αV and α5 integrins identifies MSC subpopulations of varying immunosuppressive capacity on fibrin hydrogels. A representative MSC line obtained from All Cells (BM2893) and a representative MSC line from Lonza (1F3422) were evaluated. (A) FACS plots of FACS sorted $\alpha_V^{LO}\alpha_5^{LO}$ expressing MSCs, $\alpha_V^{MED}\alpha_5^{MED}$ expressing MSCs, and $\alpha_V^{HI}\alpha_5^{HI}$ expressing MSCs and unsorted MSCs. (B and C) (B) The percent proliferating and (C) $CD25^+$ $CD4^+$ T-cells in the presence of FACS sorted or unsorted MSCs lines with IFN-γ licensing, cultured on fibrin. (D and E) (D) The percent proliferating and (E) $CD25^+$ $CD8^+$ T-cells in the presence of FACS sorted or unsorted MSCs lines with IFN-γ licensing, cultured on fibrin. Labels for groups in (B-E) are shown in (E), where 'LO' denotes $\alpha_V^{LO}\alpha_5^{LO}$ expressing MSCs, 'MED' denotes $\alpha_V^{MED}\alpha_5^{MED}$ expressing MSCs, 'HI' denotes $\alpha_V^{HI}\alpha_5^{HI}$ expressing MSCs, 'stain' denotes unsorted MSCs stained with FACS sorting antibodies, and 'unstain' denotes unsorted, unstained MSCs. Data are presented as means ± SD. Significance is denoted by $*P \leq 0.05$, $***P \leq 0.001$, or $****P \leq 0.0001$ by one-way analysis of variance (ANOVA) with Tukey's post hoc test; separate comparisons were made between conditions of each cell line.

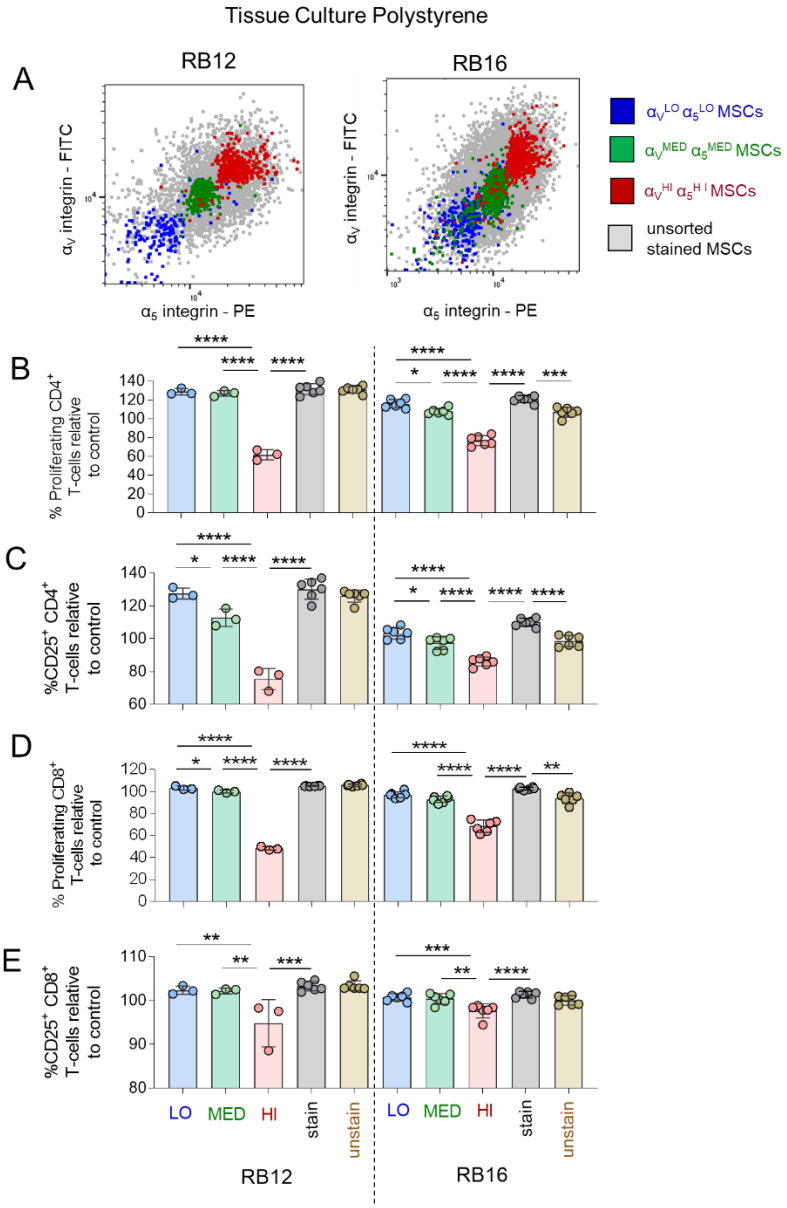

Fig. S21. Magnitude of α_V and α_5 integrins identifies MSC subpopulations of varying immunosuppressive capacity on tissue culture polystyrene. (A) FACS plots of FACS sorted $\alpha_V^{LO}\alpha_5^{LO}$ expressing MSCs, $\alpha_V^{MED}\alpha_5^{MED}$ expressing MSCs, and $\alpha_V^{HI}\alpha_5^{HI}$ expressing MSCs and unsorted MSCs. (B and C) (B) The percent proliferating and (C) $CD25^+$ $CD4^+$ T-cells in the presence of FACS sorted or unsorted MSCs lines with IFN-γ licensing, cultured on TCPS. (D and E) (D) The percent proliferating and (E) $CD25^+$ $CD8^+$ T-cells in the presence of FACS sorted or unsorted MSCs lines with IFN-γ licensing, cultured on TCPS. Labels for groups in (B-E) are shown in (E), where 'LO' denotes $\alpha_V^{LO}\alpha_5^{LO}$ expressing MSCs, 'MED' denotes $\alpha_V^{MED}\alpha_5^{MED}$ expressing MSCs, 'HI' denotes $\alpha_V^{HI}\alpha_5^{HI}$ expressing MSCs, 'stain' denotes unsorted MSCs stained with FACS sorting antibodies, and 'unstain' denotes unsorted, unstained MSCs. Data are presented as means ± SD. Significance is denoted by $*P \leq 0.05$, $**P \leq 0.01$, $***P \leq 0.001$, or $****P \leq 0.0001$ by one-way analysis of variance (ANOVA) with Tukey's post hoc test; separate comparisons were made between conditions of each cell line.

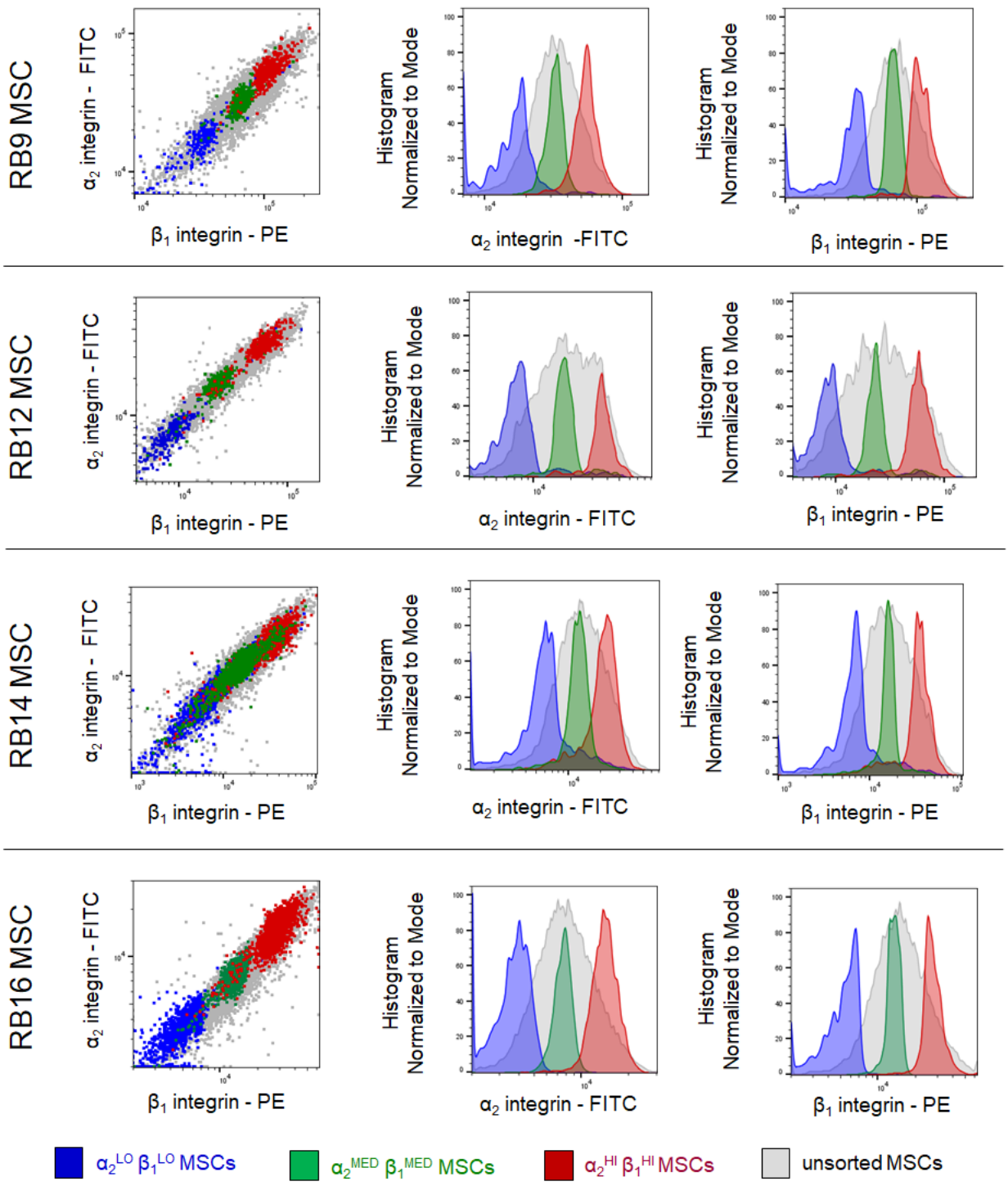

Fig. S22. FACS sorted MSCs by collagen integrins. Representative FACS plots of MSCs FACS sorted by magnitude of α_2 and β_1 integrins for each MSC cell line.

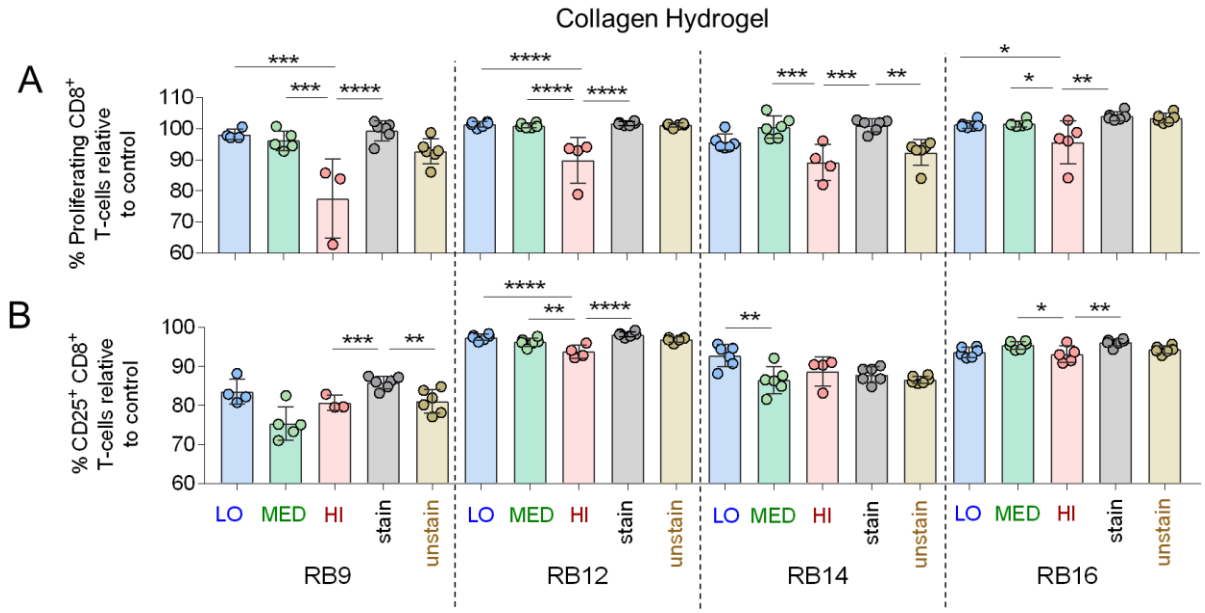

Fig. S23. Magnitude of α_2 and β_1 integrins identifies MSC subpopulations of varying immunosuppressive capacity on collagen hydrogels. (A) The percent proliferating and (B) $CD25^+$ $CD8^+$ T-cells in the presence of FACS sorted or unsorted MSCs lines with IFN-γ licensing, cultured on collagen. Labels for groups in (A-B) are shown in (B), where 'LO' denotes $\alpha_2^{LO}\beta_1^{LO}$ expressing MSCs, 'MED' denotes $\alpha_2^{MED}\beta_1^{MED}$ expressing MSCs, 'HI' denotes $\alpha_2^{HI}\beta_1^{HI}$ expressing MSCs, 'stain' denotes unsorted MSCs stained with FACS sorting antibodies, and 'unstain' denotes unsorted, unstained MSCs. n = 3-6 for all data sets. Data are presented as means ± SD. Significance is denoted by $*P \leq 0.05$, $**P \leq 0.01$, $***P \leq 0.001$, or $****P \leq 0.0001$ by one-way analysis of variance (ANOVA) with Tukey's post hoc test; separate comparisons were made between conditions of each cell line.

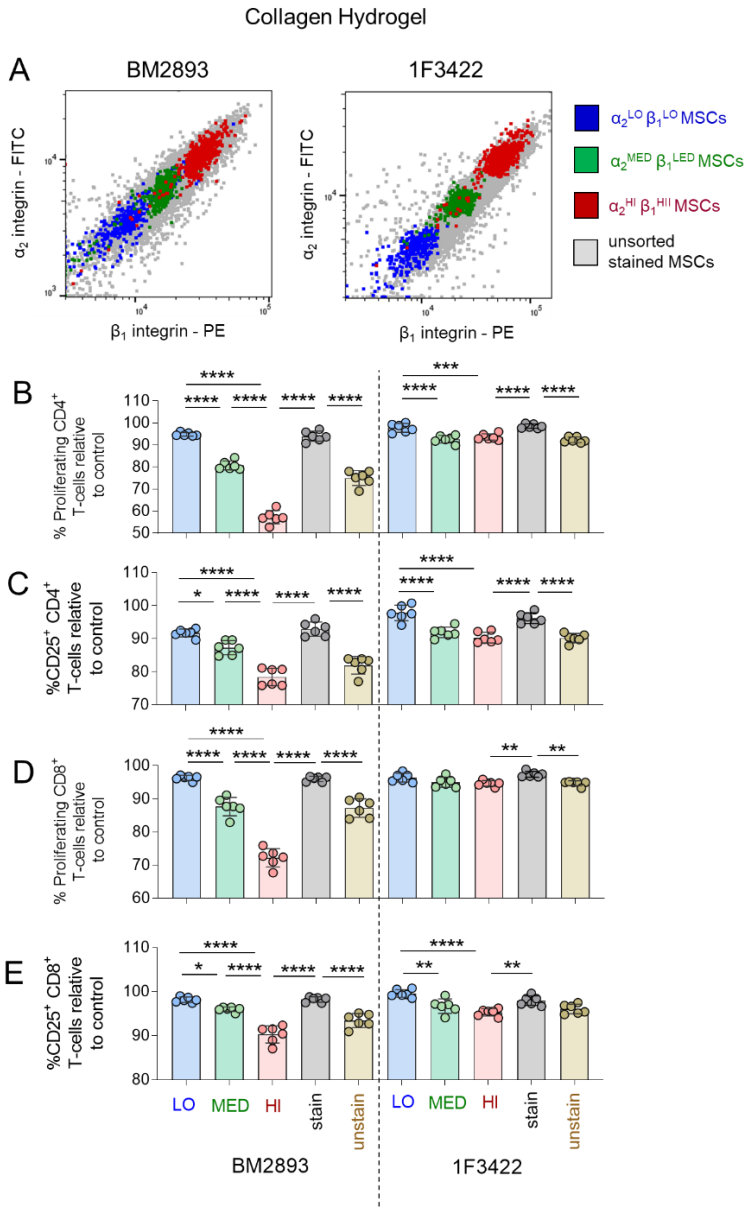

Fig. S24. Magnitude of α2 and β1 integrins identifies MSC subpopulations of varying immunosuppressive capacity on collagen hydrogels. A representative MSC line obtained from All Cells (BM2893) and a representative MSC line from Lonza (1F3422) were evaluated. (A) FACS plots of FACS sorted $\alpha_2^{LO}\beta_1^{LO}$ expressing MSCs, $\alpha_2^{MED}\beta_1^{MED}$ expressing MSCs, and $\alpha_2^{HI}\beta_1^{HI}$ expressing MSCs with unsorted MSCs. (B and C) (B) The percent proliferating and (C) $CD25^+$ $CD4^+$ T-cells in the presence of FACS sorted or unsorted MSCs lines with IFN-γ licensing, cultured on collagen. (D and E) (D) The percent proliferating and (E) $CD25^+$ $CD8^+$ T-cells in the presence of FACS sorted or unsorted MSCs lines with IFN-γ licensing, cultured on collagen. Labels for groups in (B-E) are shown in (E), where 'LO' denotes $\alpha_2^{LO}\beta_1^{LO}$ expressing MSCs, 'MED' denotes $\alpha_2^{MED}\beta_1^{MED}$ expressing MSCs, 'HI' denotes $\alpha_2^{HI}\beta_1^{HI}$ expressing MSCs, 'stain' denotes unsorted MSCs stained with FACS sorting antibodies, and 'unstain' denotes unsorted, unstained MSCs. Data are presented as means ± SD. Significance is denoted by $*P \leq 0.05$, $**P \leq 0.01$, $***P \leq 0.001$, or $****P \leq 0.0001$ by one-way analysis of variance (ANOVA) with Tukey's post hoc test; separate comparisons were made between conditions of each cell line.

Trial Number	Status	Clinical Indication	Cells	Biomaterial(s)
NCT00850187	Completed	• Knee Osteoarthritis	Autologous bone marrow derived MSCs	Collagen
NCT01159899	Unknown	• Osteoarthritis • Knee Osteoarthritis • Osteochondritis Dissecans • Osteonecrosis	Autologous bone marrow derived MSCs	Collagen
NCT01958502	Unknown	• Nonunion of Fracture	Bone marrow derived MSCs	Collagen
NCT03724617	Completed	• Thin Endometrium • Intrauterine Adhesion	Umbilical Cord MSC	Collagen
NCT03592849	Enrolling by invitation	• Infertility, female • Endometrium	Umbilical cord derived MSCs	Collagen
NCT03563495	Completed	• Cleft lip and palate	Autologous bone marrow derived MSCs	Collagen
NCT03509870	Terminated	• Diabetic Foot Ulcer	Allogenic bone marrow derived MSCs	Collagen
NCT04446884	Completed	• Stress Urinary Incontinence	Autologous adipose derived MSCs	Collagen
NCT04434794	Completed	• Gingival Recession	Autologous adipose derived MSCs	Collagen
NCT02005861	Unknown	• Osteochondritis	Bone marrow derived MSCs	Collagen
NCT02947191	Active, not recruiting	• Chronic Nasal Septum Perforation	Umbilical cord derived MSCs	Collagen
NCT02786017	Unknown	• Decompensated Cirrhosis	Umbilical cord derived MSCs	Collagen
NCT02767817	Active, not recruiting	• Brain Injury	MSCs	Collagen
NCT03294759	Active, not recruiting	• Anterior cruciate ligament rupture	Autologous bone marrow derived MSCs	Collagen
NCT02745808	Unknown	• Erectile Dysfunction • Type 1 Diabetes Mellitus • Type 2 Diabetes Mellitus	Umbilical cord derived MSCs	Collagen
NCT02672280	Unknown	• Wounds • Diabetic Foot Ulcers • Burns	Umbilical cord derived MSCs	Collagen
NCT02644447	Completed	• Premature Ovarian Failure	Allogenic umbilical cord derived MSCs	Collagen
NCT02635464	Completed	• Chronic Ischemic Cardiomyopathy	Allogenic umbilical cord derived MSCs	Collagen
NCT01687777	Unknown	• Rotator Cuff Tears	Autologous MSCs	Collagen
NCT03137979	Unknown	• Periodontitis	Gingiva MSCs	Collagen
NCT03259217	Unknown	• Diabetic Foot Ulcer	Adipose derived MSCs	Collagen-alginate with chitosan nanoparticles
NCT03766217	Completed	• Cleft Lip and Palate	Autologous deciduous dental pulp MSCs	Collagen and hydroxyapatite
NCT03070275	Completed	• Dental implant therapy	Autologous aveolar bone marrow derived MSCs	Collagen and fibrin
NCT04236739	Recruiting	• Cartilage damage	Allogenic MSCs and autologous chondrocytes	Fibrin
NCT03865394	Unknown	• Diabetic foot ulcer	Autologous adipose derived MSCs	Fibrin
NCT00891501	Unknown	• Degenerative Arthritis • Chondral Defects • Osteochondral Defects	Autologous bone marrow derived MSCs	Fibrin
NCT04210440	Completed	• Hip Necrosis • Hip Injuries	Autologous bone marrow derived MSCs	Fibrin
NCT01803347	Completed	• Anal Fistula	Autologous adipose derived MSCs	Fibrin
NCT01751282	Terminated	• Non healing wounds	Autologous bone marrow derived MSCs	Fibrin

NCT03113747	Unknown	• Second- or third- degree burns	Allogenic adipose derived MSCs	Fibrin
NCT02630836	Withdrawn	• Femoral Neck Fracture	Allogenic bone marrow derived MSCs	Fibrin
NCT02384499	Completed	• Fecal Incontinence	Allogenic adipose derived MSCs	Fibrin
NCT03449082	Active, not recruiting	• Lateral Epicondylitis	Allogenic adipose derived MSCs	Fibrin
NCT02298023	Unknown	• Rotator Cuff Tear	Allogenic adipose derived MSCs	Fibrin
NCT03766139	Unknown	• Intrabony Periodontal Defect	Peripheral Blood MSCs	Fibrin
NCT03044119	Unknown	Dental implants	Peripheral blood MSCs	Fibrin
NCT01532076	Terminated	• Osteoporotic Fractures	Adipose derived MSCs	Fibrin and hydroxyapatite microgranules
NCT03103295	Unknown	• Bone defects	Autologous bone marrow derived MSCs, periosteal progenitor cells, and peripheral blood-derived endothelial progenitor cells	Fibrin with demineralized bone matrix
NCT03102879	Completed	• Periapical Periodontitis	Umbilical cord derived MSCS	Plasma-derived biomaterial
NCT04297813	Recruiting	• Alveolar bone atrophy	Autologous MSCs	Biphasic calcium phosphate
NCT01842477	Completed	• Delayed Union After Fracture of Humerus, Tibial or Femur	Autologous bone marrow derived MSCs	biphasic calcium phosphate
NCT02751125	Completed	• Bone atrophy	Autologous bone marrow derived MSCs	Biphasic calcium phosphate
NCT03325504	Recruiting	• Non union fracture	Autologous bone marrow derived MSCs	Biphasic calcium phosphate
NCT03638154	Completed	• Periodontal intrabony defect	Gingivial MSCs and gingivial fibroblasts	Beta tri calcium phosphate
NCT01742260	Unknown	• Surgically-created Resection Cavity	Allogenic MSCs	Beta tri calcium phosphate and PLGA
NCT03798353	Recruiting	• Myocardial Infarction	Allogeneic umbilical cord Wharton´s jelly-derived adult MSCs	Decellularized human pericardial matrix
NCT02949414	Suspended	• Tracheomalacia • Tracheal Stenosis	Autologous bone marrow derived MSCs	Decellularized human tracheal scaffold
NCT02352077	Enrolling by invitation	• Spinal Cord Injury	MSC	Decellularized bovine aponeurosis
NCT04435249	Not yet recruiting	• Bronchopleural Fistula	Autologous bone marrow derived MSCs	Decellularized airway scaffold
NCT02230514	Completed	• Atrophic Nonunion of Fracture	Autologous MSCs	Decellularized bone tissue
NCT02034786	Unknown	• Lipodystrophies • Aesthetics Procedure •	Autologous adipose derived MSCs	Hyaluronic acid
NCT01981330	Completed	• Improved Healing of Scarred Vocal Folds • Improved Vocal Fold Status • Improved Vocal Fold Function	Autologous MSCs	hyaluronan gel
NCT03066245	Recruiting	• Aneurysmal Bone Cyst	Bone marrow derived MSCs	PLGA
NCT01298830	Terminated	• Intracerebral Hemorrhage (ICH)	Allogenic MSCs	Alginate

Table S1. Non-exhaustive list of clinical trials that combine MSCs with biomaterials from C*linicalTrials.gov*. Current as of May 13, 2021.

Hydrogel	Storage Modulus (G')	Loss Modulus (G")
24 mg/mL fibrinogen (fibrin gel)	282.7 ± 3.4 Pa	48.7 ± 0.9 Pa
12 mg/mL fibrinogen (fibrin gel)	119.2 ± 1.2 Pa	18.5 ± 0.9 Pa
6 mg/mL fibrinogen (fibrin gel)	49.0 ± 1.0 Pa	8.5 ± 1.1 Pa
3 mg/mL fibrinogen gel (fibrin gel)	46.4 ± 1.0 Pa	6.7 ± 1.0 Pa
6 mg/mL collagen I (collagen gel)	274.1 ± 1.0 Pa	41.0 ± 1.1 Pa
3 mg/mL collagen I (collagen gel)	89.0 ± 1.3 Pa	14.8 ± 1.0 Pa
1.5 mg/mL collagen I (collagen gel)	28.7 ± 0.9 Pa	6.8 ± 0.8 Pa
0.75 mg/mL collagen I (collagen gel)	26.2 ± 1.1 Pa	4.7 ± 1.1 Pa

Table S2. List of all tested hydrogels and their measured storage and loss modulus.

hMSC Donor ID	Sex	Age	Vendor
RB9	M	43	RoosterBio
RB12	M	33	RoosterBio
RB14	F	20	RoosterBio
RB16	F	26	RoosterBio
PCBM1632	M	24	All Cells
PCBM1662	F	31	All Cells
BM2893	M	40	All Cells
BM3018	M	41	All Cells
110877	M	22	Lonza
127756	M	43	Lonza
1F3422	M	39	Lonza
8F3560	F	24	Lonza

Table S3. List of all tested MSC cell lines with respective donor and vendor information.

Figure	MSC passage number	PBMC Donor
Fig. 2	RB9 p3, RB12 p3, RB14 p3, RB16 p3, PCBM1632 p3, PCBM1662 p3, BM2893 p3, BM3018 p3, 110877 p3, 127756 p3, 1F3422 p3, 8F3560 p3	Fig. 2A-D: Donor A Fig. 2I-L: Donor G
Fig. 3	RB9 p3, RB12 p3, RB14 p3, RB16 p3	Donor A
Fig. 4	RB9 p3, RB12 p3, RB14 p3, RB16 p3	Donor B
Fig. 5	RB9 p3, RB12 p3, RB14 p3, RB16 p3	Donor C and Donor D
Fig. 6	Fig. 6A: RB9 p3, RB12 p3, RB14 p3, RB16 p3 Fig. 6B-F: RB9 p4, RB12 p4, RB14 p2, RB16 p2	RB9 data- Donor D RB12 data- Donor D and Donor E RB14 data- Donor D and Donor E RB16 data- Donor F
Fig. 7	Fig. 7A: RB9 p3, RB12 p3, RB14 p3, RB16 p3 Fig. 7B-F: RB9 p4, RB12 p2, RB14 p2, RB16 p2	RB9 data- Donor E RB12 data- Donor F RB14 data- Donor E RB16 data- Donor F
Fig. S2	RB9 p3, RB12 p3, RB14 p3, RB16 p3, PCBM1632 p3, PCBM1662 p3, BM2893 p3, BM3018 p3, 110877 p3, 127756 p3, 1F3422 p3, 8F3560 p3	Fig. 2A-D: Donor A Fig. 2E-H: Donor G
Fig. S3	PCBM1632 p3, PCBM1662 p3, BM2893 p3, BM3018 p3, 110877 p3, 127756 p3, 1F3422 p3, 8F3560 p3	Donor L
Fig. S4	RB12 p3, RB16 p3	Donor H
Fig. S5	RB12 p3, RB16 p3	Donor H
Fig. S6	RB9 p3, RB12 p3, RB14 p3, RB16 p3, PCBM1632 p3, PCBM1662 p3, BM2893 p3, BM3018 p3, 110877 p3, 127756 p3, 1F3422 p3, 8F3560 p3	Donor G
Fig. S7	RB9 p3, RB12 p3, RB14 p3, RB16 p3	Donor A
Fig. S8	RB9 p3, RB12 p3, RB14 p3, RB16 p3	Donor B
Fig. S9	RB9 p3, RB12 p3, RB14 p3, RB16 p3	Donor C and Donor D
Fig. S10	RB12 p3, RB16 p3	
Fig. S11	RB9 p3, RB12 p3, RB14 p3, RB16 p3	Donor C and Donor D
Fig. S12	RB9 p3, RB12 p3, RB14 p3, RB16 p3	Donor C and Donor D
Fig. S13	RB12 p3, RB16 p3	
Fig. S14	RB12 p3, RB16 p3	Donor H
Fig. S15	RB12 p3, RB16 p3	
Fig. S16	RB9 p3, RB12 p3, RB14 p3, RB16 p3, PCBM1632 p3, PCBM1662 p3, BM2893 p3, BM3018 p3, 110877 p3, 127756 p3, 1F3422 p3, 8F3560 p3	
Fig. S17	RB9 p3, RB12 p3, RB14 p3, RB16 p3, PCBM1632 p3, PCBM1662 p3, BM2893 p3, BM3018 p3, 110877 p3, 127756 p3, 1F3422 p3, 8F3560 p3	Donor G
Fig. S18	RB9 p4, RB12 p4, RB14 p2, RB16 p2	
Fig. S19	RB9 p4, RB12 p4, RB14 p2, RB16 p2	RB9 data- Donor D RB12 data- Donor D and Donor E RB14 data- Donor D and Donor E RB16 data- Donor F
Fig. S20	BM2893 p3, 1F3422 p5	BM2893 Data- Donor J 1F3422 Data- Donor L
Fig. S21	RB12 p3, RB16 p2	RB12 data- Donor H RB16 data- Donor I

Fig. S22	RB9 p4, RB12 p2, RB14 p2, RB16 p2	
Fig. S23	RB9 p4, RB12 p2, RB14 p2, RB16 p2	RB9 data- Donor E RB12 data- Donor F RB14 data- Donor E RB16 data- Donor F
Fig. S24	BM2893 p3, 1F3422 p3	Donor K

Table S4. List of MSC cell lines, respective MSC passage numbers, and PBMC donors used for each figure.